UC Irvine
UC Irvine Previously Published Works

Title

Interaction of histone H4 with Cse4 facilitates conformational changes in Cse4 for its sumoylation and mislocalization.

Permalink

https://escholarship.org/uc/item/3vh22214

Journal

Nucleic Acids Research, 52(2)

Authors

Ohkuni, Kentaro

Au, Wei-Chun

Kazi, Amira

et al.

Publication Date

2024-01-25

DOI

10.1093/nar/gkad1133

Peer reviewed

eScholarship.org Powered by the California Digital Library
University of California

Nucleic Acids Research, 2024, **52**, 643–659
https://doi.org/10.1093/nar/gkad1133
Advance access publication date: 1 December 2023
Gene regulation, Chromatin and Epigenetics

Interaction of histone H4 with Cse4 facilitates conformational changes in Cse4 for its sumoylation and mislocalization

Kentaro Ohkuni[1,†], Wei-Chun Au[1,†], Amira Z. Kazi[1], Mark Villamil[2], Peter Kaiser[2] and Munira A. Basrai[1,*]

[1]Genetics Branch, Center for Cancer Research, National Cancer Institute, National Institutes of Health, Bethesda, MD 20892, USA
[2]Department of Biological Chemistry, School of Medicine, Center for Epigenetics and Metabolism, Chao Family Comprehensive Cancer Center, University of California, Irvine, CA 92697-1700, USA

[*]To whom correspondence should be addressed. Tel: +1 240 760 6746; Fax: +1 240 541 4529; Email: basraim@nih.gov
[†]The first two authors should be regarded as Joint First Authors.

Abstract

Mislocalization of overexpressed CENP-A (Cse4 in budding yeast, Cnp1 in fission yeast, CID in flies) contributes to chromosomal instability (CIN) in yeasts, flies, and human cells. Mislocalization of CENP-A is observed in many cancers and this correlates with poor prognosis. Structural mechanisms that contribute to mislocalization of CENP-A are poorly defined. Here, we show that interaction of histone H4 with Cse4 facilitates an *in vivo* conformational change in Cse4 promoting its mislocalization in budding yeast. We determined that Cse4 Y193A mutant exhibits reduced sumoylation, mislocalization, interaction with histone H4, and lethality in *psh1Δ* and *cdc48-3* strains; all these phenotypes are suppressed by increased gene dosage of histone H4. We developed a new *in vivo* approach, antibody accessibility (AA) assay, to examine the conformation of Cse4. AA assay showed that wild-type Cse4 with histone H4 is in an 'open' state, while Cse4 Y193A predominantly exhibits a 'closed' state. Increased gene dosage of histone H4 contributes to a shift of Cse4 Y193A to an 'open' state with enhanced sumoylation and mislocalization. We provide molecular insights into how Cse4-H4 interaction changes the conformational state of Cse4 *in vivo*. These studies advance our understanding for mechanisms that promote mislocalization of CENP-A in human cancers.

Graphical abstract

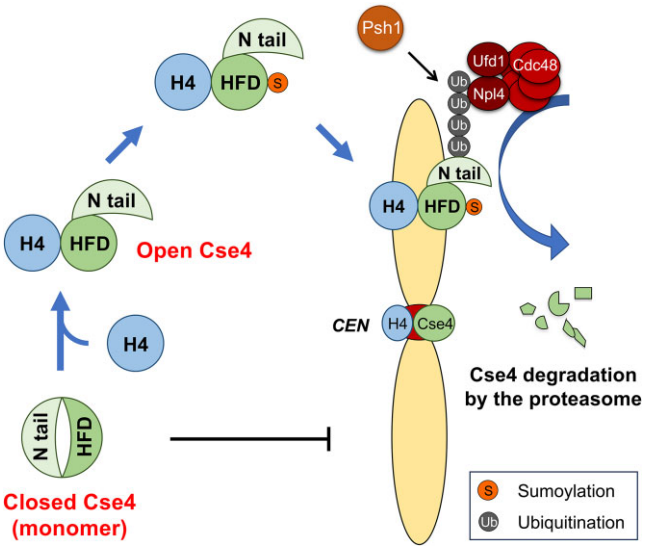

Introduction

Chromosomal instability (CIN) and aneuploidy are hallmarks of cancer cells. Centromeric (*CEN*) DNA and associated proteins referred to as kinetochore are key determinants to prevent CIN and aneuploidy. The kinetochore provides an attachment site for microtubules for segregation of sister chromatids during mitosis. Centromeric localization of evolutionarily conserved histone H3 variant CENP-A (Cse4 in *Saccharomyces cerevisiae*, Cnp1 in *Schizosaccharomyces pombe*, CID in *Drosophila melanogaster*) is a platform for kinetochore assembly (1–3). In budding yeast, Cse4 forms the specialized single nucleosome (referred to

Received: August 23, 2023. **Revised:** October 27, 2023. **Editorial Decision:** November 1, 2023. **Accepted:** November 9, 2023
Published by Oxford University Press on behalf of Nucleic Acids Research 2023.
This work is written by (a) US Government employee(s) and is in the public domain in the US.

as point centromere), whereas human CENP-A nucleosomes are composed of repetitive DNA elements located on 1- to 4- Mb chromosomal regions (referred to as regional centromere) (1–3). The evolutionarily conserved CENP-A specific histone chaperone Scm3/CAL1/HJURP (Holliday Junction Recognition Protein) regulates the centromeric localization of Cse4/Cnp1/CID/CENP-A in budding and fission yeasts, flies and humans, respectively (4–11). Overexpression of CENP-A and its homologs leads to its mislocalization to non-centromeric chromatin and increased CIN in budding and fission yeasts, flies, and humans (12–19). Overexpression and mislocalization of CENP-A is observed in many cancers, which correlates with poor patient survival and increased risk of disease progression (20–27). Defining mechanisms that prevent or contribute to the mislocalization of overexpressed Cse4/CENP-A is critical for understanding how mislocalization of Cse4/CENP-A contributes to aneuploidy in cancers.

Studies with *S. cerevisiae* have shown that ubiquitin-mediated proteolysis is one of the key mechanisms to regulate soluble pools and chromatin-bound of Cse4, which contribute to preventing Cse4 mislocalization to non-centromeric regions. Multiple E3 ubiquitin ligases such as Psh1 (28,29), Slx5 (30–32), Ubr1 (31), Skp-Cullin-F-box (SCF)-Rcy1 (33) and SCF-Met30/Cdc4 (34) regulate cellular levels of Cse4 to prevent Cse4 mislocalization. We recently showed that Psh1 contributes to the polyubiquitination of mislocalized Cse4, which is evicted by Cdc48 segregase under normal physiological conditions (35). Psh1-mediated proteolysis of Cse4 is regulated by several factors such as proline isomerase Fpr3 (36), FACT (Facilitates Chromatin Transcription/Transactions) complex (37), CK2 (casein kinase 2) (38), HIR histone chaperone complex (39), and DDK (Dbf1-dependent kinase) complex (40) under overexpressed Cse4. We and others have shown that overexpression of Cse4 leads to enhanced lethality and mislocalization of Cse4 to non-centromeric regions in *psh1Δ, cdc48-3, met30-6, cdc4-1, slx5Δ, cdc7-4* and *hir2Δ* strains (28–30,34,35,39,40). In general, mutation and deletion of factors that prevent Cse4 mislocalization show synthetic dosage lethality (SDL) when Cse4 is overexpressed from a galactose-inducible promoter (*GAL-CSE4*).

Characterization of pathways that contribute to the mislocalization of Cse4 is also an area of active research. The evolutionarily conserved replication dependent Chromatin Assembly Factor 1 (CAF-1) promotes mislocalization of overexpressed Cse4 in budding yeast (41). Our studies have defined a key role for sumoylation of Cse4 in regulating its mislocalization to non-centromeric regions and leading to SDL in *psh1Δ GAL-CSE4* and *cdc48-3 GAL-CSE4* strains (35,42,43). We have shown that: (i) sumoylation of lysine (K) 215/216 promotes mislocalization of Cse4 and SDL in *psh1Δ GAL-CSE4* and *cdc48-3 GAL-CSE4* strains (35,42). However, structural effects independent of sumoylation also play a role in mislocalization of Cse4 because K-to-A substitution in *GAL-cse4 K215A/216A* displays significantly reduced lethality and mislocalization of Cse4 as compared to that observed for *GAL-cse4 K215R/216R* (structurally mimetic mutant that cannot be sumoylated) (42), (ii) Strains with reduced gene dosage of histone H4 (*hhf1Δ* or *hhf2Δ*) exhibit defects in Cse4 sumoylation, reduced mislocalization of Cse4, and lack of SDL in *psh1Δ GAL-CSE4* and *cdc48-3 GAL-CSE4* strains (35,43), (iii) Cse4 Y193A exhibits defects in sumoylation and does not lead to SDL in *psh1Δ* and *cdc48-3* strains, whereas the structural mimetic Cse4 Y193F is sumoylated and exhibits SDL in the *psh1Δ* and *cdc48-3* strains (35,43) and (iv) Cse4–H4 dimer defective mutants such as *cse4-102*, *cse4-111* and *hhf1-20* show defects in sumoylation and do not lead to *psh1Δ GAL-CSE4* SDL (43). Based on these results, we hypothesized that the interaction of Cse4 with histone H4 facilitates an *in vivo* structural conformation of Cse4 which is critical for Cse4 sumoylation, mislocalization, and *GAL-CSE4* SDL in *psh1Δ* and *cdc48-3* strains. Notably, *in vitro* studies by Malik *et al.* (44) showed that monomer Cse4 exists in a 'closed' conformation due to an interdomain interaction of the N- and C-terminus of Cse4; binding of Cse4 with histone H4 facilitates an 'open' state of Cse4.

In this study, we used Cse4 Y193A as a tool to examine how Cse4–H4 interaction affects the structural conformation of Cse4 *in vivo* and the consequences of the structure on sumoylation and mislocalization of Cse4 to non-centromeric regions. Cse4 Y193 is located at the center of alpha helix 2 and interacts with the alpha helix 2 of histone H4 (45). We determined that the Cse4 Y193A mutant exhibits reduced sumoylation and mislocalization, as well as defects in the interaction with histone H4 *in vivo*. Increased gene dosage of histone H4 facilitates Cse4 Y193A–H4 interaction, sumoylation, protein stability, and mislocalization of Cse4 Y193A to non-centromeric regions. We developed a new *in vivo* approach, antibody accessibility (AA) assay, to show that wild-type Cse4 and structurally mimetic mutant Cse4 Y193F are in an 'open' state, whereas Cse4 Y193A is in a 'closed' state. Cse4 Y193A exhibits an 'open' state upon increased dosage of wild-type histone H4, but not mutant *hhf2-20*, which is defective for interaction with Cse4. Our results provide the first evidence showing that Cse4-H4 interaction contributes to an 'open' conformation of Cse4 *in vivo*, thereby facilitating sumoylation and mislocalization of Cse4.

Materials and methods

Yeast strains, plasmids and methods

Supplementary Tables S1 and S2 describe the genotype of yeast strains and plasmids used for this study, respectively. Gene deletions and epitope-tagged alleles were constructed at the endogenous loci using standard PCR-based integration. All epitope tagging was confirmed by Western blot analysis.

Yeast cells were grown in/on rich media (YPD: 1% yeast extract, 2% bacto-peptone, 2% glucose) or synthetic complete (SC) media containing 2% glucose, 2% raffinose, 2% galactose or 2% raffinose + 2% galactose.

In vivo sumoylation assay and co-immunoprecipitation (co-IP)

Cells were grown to logarithmic phase of growth in a 2% raffinose synthetic medium selective for the plasmids at 25°C. Galactose was added to the media to a final concentration of 2% to induce Cse4 expression from the *GAL* promoter for 3–4 h. Cells (50 OD_{600}) were pelleted, rinsed with sterile water, and suspended in 0.5 ml of guanidine buffer (0.1 M Tris [pH 8.0], 6.0 M guanidine chloride, 0.5 M NaCl) for sumoylation assay, or 0.5 ml of IP lysis buffer (100 mM Tris [pH 7.5], 150 mM NaCl, 0.1 mM EDTA, 1 mM DTT, 0.5% NP-40, 10% glycerol, 1 mM PMSF, and protease inhibitor cocktail (Sigma, P8215)) for co-IP. Cells were homogenized with Matrix C (MP Biomedicals) using a bead beater (MP Biomedicals, FastPrep-24 5G). Cell lysates were clarified by centrifu-

gation at 6000 rpm for 5–7 min and protein concentration was determined using a DC protein assay kit (Bio-Rad). Samples containing equal amounts of protein were brought to a total volume of 1 ml with appropriate buffer.

In vivo sumoylation was assayed in crude yeast extracts using nickel-nitrilotriacetic acid (Ni-NTA) agarose beads to pull down His-HA-tagged Cse4 as described previously (46) with modifications. Cell lysates were incubated with 100 µl of Ni-NTA superflow beads (Qiagen, 30430) overnight at 4°C. After being washed with guanidine buffer one time and with breaking buffer (0.1 M Tris [pH 8.0], 20% glycerol, 1 mM PMSF) five times, beads were incubated with 2× Laemmli buffer including imidazole at 100°C for 5 min. Co-IPs were performed in crude yeast extracts using anti-HA agarose (A2095, Sigma) overnight at 4°C. After being washed with Tris-buffered saline with Tween-20 (TBS-T) three times, beads were incubated with 2x Laemmli buffer at 100°C for 5 min.

The protein samples were resolved on a 4–12% Bis–Tris gel (Novex, NP0322BOX), proteins were transferred onto nitrocellulose membrane, and Western blotting was performed according to standard protocol. Antibodies were as follows: anti-HA (12CA5) mouse (Roche, 11583816001), anti-Smt3 (y-84) (Santa Cruz Biotechnology, sc-28649), and anti-H4 rabbit (Abcam, ab10158). Protein levels were quantified using Image Lab software (version 6.0.0) from Bio-Rad Laboratories, Inc (Hercules, CA) or Gene Tools software (version 3.8.8.0) from SynGene (Frederick, MD).

Subcellular fractionation assay

Cells were grown to logarithmic phase of growth in 2% glucose (for endogenous Cse4) or 2% raffinose (for *GAL-CSE4*)-containing synthetic medium selective for the plasmids at 25°C. Galactose was added to the media to a final concentration of 2% to induce Cse4 expression from the *GAL* promoter for 4 h. Subcellular fractionation was performed using 50 OD_{600} cells as described previously (15). The protein samples were analyzed by SDS-PAGE and western blot using anti-HA (12CA5) mouse (Roche, 11583816001) and anti-H2B rabbit (Abcam, ab1790) antibodies. Protein levels were quantified using Image Lab software (version 6.0.0) from Bio-Rad Laboratories, Inc (Hercules, CA).

Protein stability assay

Protein stability assay was performed as described previously (15). Cells were grown to logarithmic phase of growth in a 2% raffinose synthetic medium selective for the plasmids at 25°C. Galactose was added to the media to a final concentration of 2% to induce Cse4 expression for 3 h. Cycloheximide (CHX) and glucose were then added to final concentrations of 10 µg/ml and 2%, respectively. Samples were taken at the indicated time points. The protein samples were analyzed by SDS-PAGE and western blot using anti-HA (12CA5) mouse (Roche, 11583816001), anti-Tub2 rabbit (Basrai laboratory), and anti-H4 rabbit (Abcam, ab10158) antibodies. Protein levels were quantified using Gene Tools software (version 3.8.8.0) from SynGene (Frederick, MD).

ChIP-qPCR

Chromatin immunoprecipitations were performed as previously described (43) with modifications. Briefly, logarithmic phase cultures were grown in galactose/raffinose (2% final concentration each) media for 3–3.5 h and were treated with formaldehyde (1%) for 20 min at 30°C. Cell pellets were washed twice in 1× PBS and 0.9 ml FA Lysis Buffer (1 mM EDTA pH8.0, 50 mM HEPES–KOH pH7.5, 140 mM NaCl, 0.1% sodium deoxycholate, 1% Triton X-100) with protease inhibitor cocktail and PMSF (1 mM) was added to resuspend the cell pellets, followed by lysis in a FastPrep-24 5G (MP Biosciences) for 40 s ten times with rest on ice between every three consecutive beads-beating. The resulting chromatin pellet was resuspended in 1.4 ml of FA Lysis Buffer and sonicated on ice with a Branson digital sonifier 24 times at 20% amplitude with a repeated 15 s on/off cycle. After 10 min of centrifugation (12 000 rpm, 4°C), 60 µl of the resulting solubilized chromatin was taken as Input and the 720 µl was used for immunoprecipitation with anti-HA-agarose beads (Sigma, A2095) overnight at 4–8°C. The beads were washed sequentially in 1 ml FA, FA-HS (500 mM NaCl), RIPA, and TE buffers for 5 min on a rotor two times each. The beads were suspended in ChIP Elution Buffer (25 mM Tris–HCl pH7.6, 100 mM NaCl, 0.5% SDS) and incubated at 65°C overnight. The supernatants were treated with proteinase K (0.5 mg/ml) and incubated at 50°C for 2 h followed by phenol/chloroform extraction and ethanol precipitation. The DNA pellet was resuspended in a total of 500 and 100 µl sterile water for Input and IP, respectively. Samples were analyzed by quantitative PCR (qPCR) performed with the 7500 Fast Real Time PCR System with Fast SYBR Green Master Mix (Applied Biosystems). The occupancy of the respective protein was calculated as % input. Primers used for this study are listed in Supplementary Table S3.

Ubiquitin (Ub) pull-down assay

Cells were grown to logarithmic phase of growth in a 2% glucose synthetic medium selective for the plasmids at 25°C. Ub pull-down assay was performed using whole cell extracts from 50 OD_{600} cells as described previously (35). The protein samples were analyzed by SDS-PAGE and western blot using anti-HA (12CA5) mouse (Roche, 11583816001) and anti-Tub2 rabbit (Basrai laboratory) antibodies.

Antibody accessibility (AA) assay

Cells were grown to logarithmic phase in a 2% raffinose synthetic medium selective for the plasmids at 25°C. Galactose was added to the media to a final concentration of 2% to induce Cse4 expression for 4 h. Cells (50 OD_{600}) were pelleted, rinsed with sterile water, and suspended in 0.5 ml of lysis buffer (50 mM Tris [pH 8.0], 5 mM EDTA, 1% Triton X-100, 150 mM NaCl, 50 mM NaF, 10 mM β-glycerophosphate, 1 mM PMSF, protease inhibitor cocktail). Cells were homogenized with Matrix C (MP Biomedicals) using a bead beater (MP Biomedicals, FastPrep-24 5G) for 40 s two times. Cell lysates were clarified by centrifugation at 6000 rpm for 5 min and protein concentration was determined using a DC protein assay kit (Bio-Rad). Samples containing 2 mg of total proteins were brought to a total volume of 1 ml with lysis buffer.

Cell lysates were incubated with 25 µl of anti-HA-Agarose antibody (Sigma, A2095) overnight at 4°C. Proteins bound to the beads were washed with lysis buffer three times (10 min each) and eluted in 2× Laemmli buffer at 100°C for 5 min. The protein samples were resolved on a 4–12% Bis–Tris gel (Novex, NP0322BOX). Cse4 levels in whole cell extracts or IP were detected by Western blot using anti-HA rabbit antibody (Sigma, H6908). Protein levels were quantified using Image Lab software (version 6.0.0) from Bio-Rad Laboratories, Inc (Hercules, CA).

Protein purifications: Cse4, Cse4 Y193A and histone H4

Yeast histone H4 was subcloned by PCR into the pET15(b) vector. Yeast Cse4 and Cse4 Y193A were subcloned by PCR into a modified pET28(a) vector with an N-terminal Avi-Smt3 tag and using the C-terminal 6xHis tag. For protein production, the H4 construct was transformed into Rosetta (DE3) cells. The cells were grown in LB media at 37°C with antibiotics chloramphenicol and ampicillin to an OD_{600} ∼0.4, the temperature was reduced to 16°C and expression was induced with 0.5 mM IPTG overnight. For the Cse4 constructs, they were transformed into BL21(DE3) cells with pBirAcm plasmid encoding BirA for biotinylation of the Avi tag. The cells were grown in LB media at 37°C with antibiotics kanamycin and chloramphenicol with the addition of 5 μg/ml biotin to an OD_{600} ∼0.4, the temperature was reduced to 16°C and expression was induced with 0.5 mM IPTG overnight. Cells were harvested and resuspended in lysis buffer (50 mM tris, 250 mM NaCl, 1 mM TCEP, 2 mM PMSF, 10 mM imidazole, and 0.1% Triton X-100, pH 8.0), sonicated on ice, and the lysate was centrifuged (12 000 rpm, Avanti JXN-26) at 4°C for 20 min. The supernatant was incubated with Ni Sepharose 6 Fast Flow resin (Cytiva) for 1 h at 4°C with constant gentle tumbling. The Ni Sepharose was loaded on a gravity column and washed with buffer containing 50 mM Tris (pH 8.0), 250 mM NaCl, 1 mM TCEP and 20 mM imidazole. Recombinant proteins were eluted with 50 mM Tris (pH 8.0), 250 mM NaCl, 1 mM TCEP and 250 mM imidazole. Protein samples were separated on a 14% SDS-PAGE and transferred to Immobilon-P Transfer Membrane (Millipore), amido black staining was used to determine purity, streptavidin-HRP was used to detect biotin incorporation in the Cse4 constructs, and anti-His was used to detect the H4.

Biolayer interferometry

Binding affinity of H4 to the Cse4 constructs was determined on Octet RED96 (Sartorus). Protein samples were diluted in either standard assay buffer (50 mM Tris, 150 mM NaCl, 0.01 mg/ml BSA, and 0.02% Tween 20, pH7.5) or high salt with reducing reagent assay buffer (50 mM Tris, 500 mM NaCl, 0.01 mg/ml BSA, 1 mM DTT and 0.02% Tween 20, pH7.5) as follows: Cse4 constructs 20 μg/ml, biocytin (quenching solution) 5 μg/ml and the H4 was diluted in a range between 50 and 0.068 μM. Octet SA Biosensors (Sartorus) were hydrated with the assay buffer prior to the experiment. The monitoring conditions were as follows: initial baseline for 60 s, loading for 120 s, quenching for 120 s, baseline for 30 s, association for 60 s, and dissociation for 90 s; shake speed 1000 rpm, and plate temperature remained at a constant 30°C. To ascertain the binding constants, the data were analyzed using Octet Data Analysis 10.0.1.6. To calculate the binding constants the following concentration of H4 was used: 50, 16.66, 5.55, 1.8, 0.617, 0.205 and 0.068 μM.

Results

Increased gene dosage of histone H4 enhances sumoylation of Cse4 Y193A, and SDL phenotype of *GAL-cse4 Y193A* in wild-type and *psh1*Δ strains

To investigate mechanisms for Cse4 mislocalization, we focused on a *cse4 Y193A* mutant (Cse4 Y193 mutated to A193). Cse4 Y193A expressed from its own promoter complements a *cse4*Δ mutant and does not show temperature sensitivity (35), and endogenous Cse4 Y193A associates with *CEN* DNA (Supplementary Figure S1). Cse4 Y193A is ideally suited to study mechanisms that contribute to Cse4 mislocalization because overexpressed Cse4 Y193A exhibits defects in sumoylation, reduced enrichment in chromatin, and lack of SDL in *psh1Δ* and *cdc48-3* strains (35,43), all of which correlate with reduced mislocalization of Cse4. Y193 of Cse4 has been proposed to interact with the alpha helix 2 of histone H4 (45). We therefore used genetic and biochemical approaches to examine whether defects in Cse4 Y193A–H4 interaction contribute to phenotypes of overexpressed Cse4 Y193A.

In budding yeast, two loci *HHF1* and *HHF2* encode identical histone H4 protein. We examined whether increased gene dosage of histone H4 (*HHF1/2μ* or *HHF2/2μ*) can lead to SDL of *psh1Δ GAL-cse4 Y193A* strain. *HHF1/2μ* and *HHF2/2μ* strains do not show growth defects on glucose plates (Figure 1A). SDL was observed for *psh1*Δ *GAL-CSE4* strain with vector, *HHF1/2μ*, or *HHF2/2μ* (Figure 1A and Supplementary Figure S2A). *GAL-cse4 Y193A* did not show SDL in a *psh1*Δ strain, however, *psh1Δ GAL-cse4 Y193A* strain with *HHF1/2μ* or *HHF2/2μ* exhibits SDL phenotype on galactose plates (Figure 1A and Supplementary Figure S2A).

We previously reported a correlation of Cse4 sumoylation to SDL phenotype (42,43). Hence, we examined whether increased gene dosage of histone H4 that contributes to *psh1Δ GAL-cse4 Y193A* SDL is due to increased Cse4 Y193A sumoylation. Sumoylation assays were done using a wild-type strain with Cse4 or Cse4 Y193A expressing vector, *HHF1/2μ* or *HHF2/2μ*. Consistent with our previous study (43), we observed greatly reduced levels of Cse4 Y193A sumoylation (Figure 1B and Supplementary Figure S3). Increased gene dosage of histone H4 led to a significant increase in the sumoylation of both wild-type Cse4 and Cse4 Y193A (Figure 1B). More importantly, the sumoylation levels of Cse4 Y193A with *H4/2μ* were about eight times higher than that observed for wild-type Cse4 vector control (Figure 1C).

The enhancement of Cse4 and Cse4 Y193A sumoylation with *H4/2μ* prompted us to examine whether expression of *HHF2/2μ* contributes to increased lethality of *GAL-CSE4* and *GAL-cse4 Y193A* in a wild-type strain. A control strain expressing *HHF2/2μ* alone did not show growth defects on glucose and galactose plates (Figure 1D). Consistent with our hypothesis, *GAL-CSE4* and *GAL-cse4 Y193A* strains expressing *HHF2/2μ* showed more severe growth defects (Figure 1D and Supplementary Figure S2B). Not surprisingly, the SDL phenotype was more pronounced for the *GAL-CSE4 HHF2/2μ* strain (Figure 1D). Taken together, our results show that increased gene dosage of histone H4 enhances sumoylation of Cse4 Y193A and results in an SDL phenotype of *GAL-cse4 Y193A* in wild-type and *psh1*Δ strains.

Increased gene dosage of histone H4 contributes to chromatin enrichment and mislocalization of Cse4 Y193A

Several studies have shown a correlation between SDL with enrichment of Cse4 in chromatin, increased Cse4 protein stability and mislocalization of Cse4 (28–30,34,35,39,40,42,43). Hence, we examined these phenotypes of strains with *GAL-cse4 Y193A* with and without *HHF2/2μ*. Subcellular fractionation showed that levels of chromatin-associated Cse4

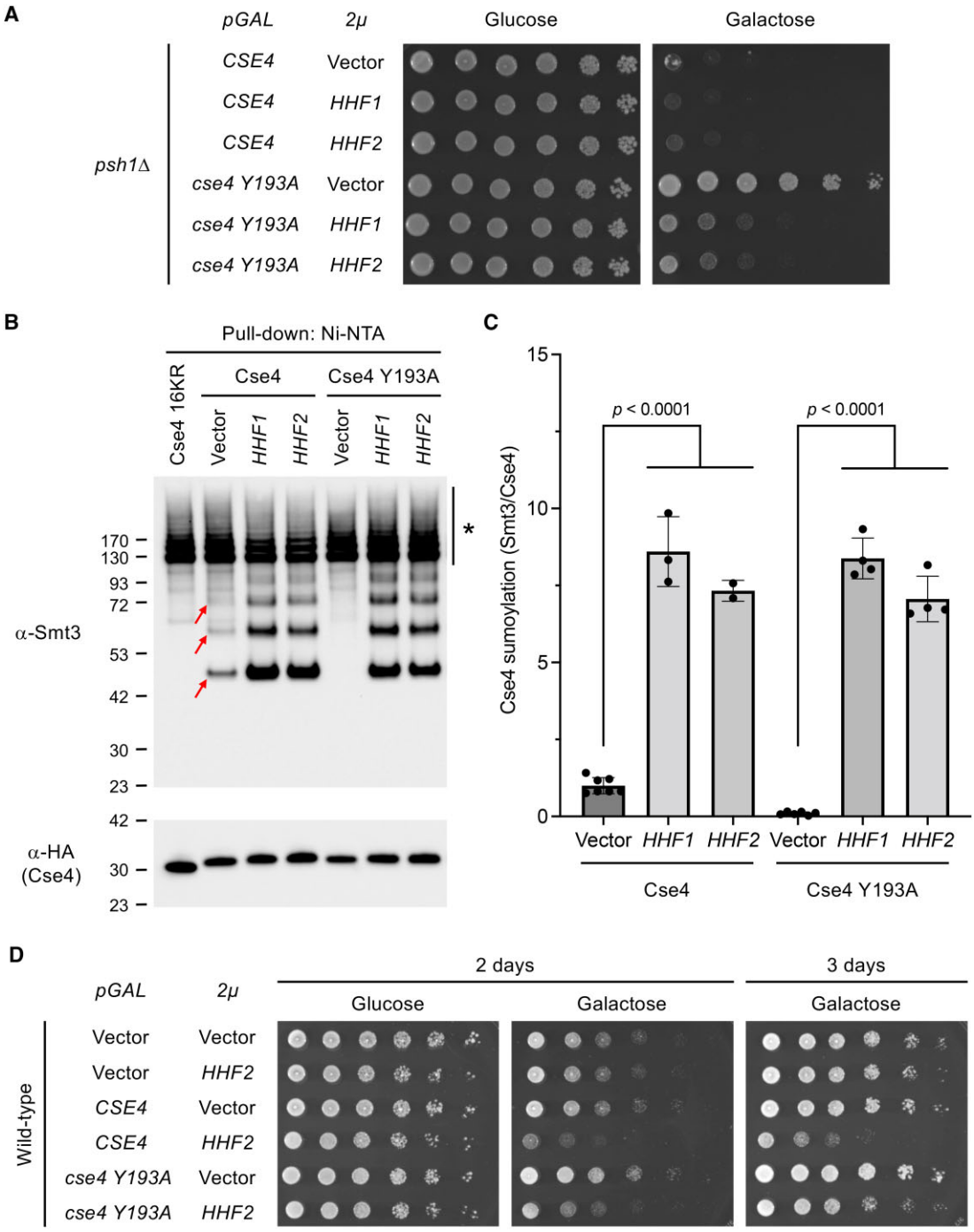

Figure 1. Increased gene dosage of histone H4 suppresses the defects in Cse4 Y193A sumoylation and leads to SDL of *psh1*Δ *GAL-cse4 Y193A* strain. (**A**) Expression of histone H4/2μ contributes to SDL phenotype in a *GAL-cse4 Y193A psh1*Δ strain. Growth assays were performed by plating five-fold serial dilution of cells on glucose (2%)- or galactose (2%)-containing synthetic medium selective for the plasmids. The plates were incubated at 25°C for 3 days. Isogenic yeast strains used here were as follows: *psh1*Δ strain (YMB9034) transformed with *GAL-CSE4* (pMB1345) or *GAL-cse4 Y193A* (pMB1766) and subsequently transformed with empty vector (pRS425), *HHF1/2μ* (pMB1928), or *HHF2/2μ* (pMB1929). (**B**) Increased gene dosage of histone H4 enhances Cse4 Y193A sumoylation. Levels of sumoylated Cse4 were assayed from the indicated strains, which were grown in galactose medium for 4 h at 25°C. Arrows indicate the three high molecular weight bands that represent sumoylated Cse4. Cse4 16KR, in which all 16 lysine (K) residues are mutated to arginine (R), is used as a negative control. Asterisk indicates nonspecific sumoylated proteins that bind to beads. Isogenic yeast strains used here were as follows: wild-type strain (BY4741) transformed with *GAL-CSE4* (pMB1345), *GAL-cse4 16KR* (pMB1344), or *GAL-cse4 Y193A* (pMB1766) and subsequently transformed with empty vector (pRS425), *HHF1/2μ* (pMB1928), or *HHF2/2μ* (pMB1929). (**C**) Quantification of relative levels of sumoylated Cse4 or Cse4 Y193A from 1B. Levels of sumoylated Cse4 were normalized to nonmodified Cse4 probed by anti-HA antibody in the pull-down samples. Statistical significance from multiple biological repeats was assessed by one-way ANOVA (p-value < 0.0001) followed by Tukey post-test (all pairwise comparisons of means). Error bars indicate standard deviation from the mean. (**D**) Expression of histone H4/2μ contributes to increased growth defects of *GAL-CSE4* and *GAL-cse4 Y193A* in a wild-type strain. Growth assays were performed by plating five-fold serial dilution of cells on glucose (2%)- or galactose (2%)-containing synthetic medium selective for the plasmids. The plates were incubated at 25°C for 2–3 days. Isogenic yeast strains used here were as follows: wild-type strain (BY4741) transformed with empty vector (pYES2 or pMB433), *GAL-CSE4* (pMB1345), or *GAL-cse4 Y193A* (pMB1766) and subsequently transformed with empty vector (pRS425) or *HHF2/2μ* (pMB1929).

Y193A were reduced when compared to wild-type Cse4 (Figure 2A and B, and Supplementary Figure S4). Increased gene dosage of histone H4 (*HHF2/2μ*) showed an enrichment of chromatin-associated Cse4 Y193A (Figure 2A and B, and Supplementary Figure S4). Consistent with these results, Cse4 Y193A was rapidly degraded after cycloheximide treatment in a wild-type strain, but more stable in strains with *HHF2/2μ* (Figure 2C and D). While the levels of histone H4 were consistent throughout the time course in both strains (Figure 2C), the initial levels of histone H4 (0 min) in cells expressing *HHF2/2μ* were slightly higher when compared to endogenous histone H4 (Figure 2E).

We next examined whether increased gene dosage of histone H4 contributes to increased stability and mislocalization of Cse4 Y193A in a *psh1Δ* strain. Similar to results with wild-type strain, Cse4 Y193A was rapidly degraded in a *psh1*Δ strain (Supplementary Figure S5), and expression of *HHF2/2μ* increased the stability of Cse4 Y193A in this strain (Figure 2F and G). Levels of histone H4 were also consistent throughout the time course in the *psh1*Δ strains (Figure 2F). Initial levels of histone H4 (0 min) in cells expressing *HHF2/2μ* were also slightly higher when compared to endogenous histone H4 (Figure 2H). The reduced stability of Cse4 Y193A even in a *psh1*Δ strain *in vivo* is due to other E3 ubiquitin ligases-mediated or ubiquitin-independent proteolysis. We next performed chromatin immunoprecipitation (ChIP)-qPCR experiments in a *psh1*Δ strain to examine the localization of Cse4 Y193A at non-centromeric regions. The advantage of using a *psh1Δ* strain for ChIP experiments is because the non-centromeric regions of Cse4 mislocalization such as promoters of *SAP4* and *RDS1*, the pericentromeric R1 region of *CEN3*, and the *ACT1* coding region are well defined based on previous studies (43,47). An enrichment of wild-type Cse4 and structural mimic mutant Cse4 Y193F was observed at these regions (Supplementary Figure S6). However, levels of Cse4 Y193A were lower at these non-centromeric regions. Strains expressing *HHF2/2μ* showed increased mislocalization of Cse4 Y193A to non-centromeric regions (Figure 2I). Taken together, we conclude that increased gene dosage of histone H4 facilitates mislocalization of Cse4 Y193A to non-centromeric regions, which consequently contributes to its increased stability.

Increased gene dosage of histone H4 facilitates Cse4 Y193A–H4 interaction

We hypothesized that the phenotypes of Cse4 Y193A with *HHF2/2μ* such as SDL, protein stability, enrichment in chromatin, and increased mislocalization are due to increased interaction of Cse4 Y193A with histone H4. Co-immunoprecipitation (Co-IP) experiments were done with strains co-expressing either *GAL-3HA-CSE4* or *GAL-3HA-cse4 Y193A* with or without *HHF2/2μ*. Immunoprecipitation with anti-HA antibody showed that Cse4 interacts with histone H4, and this interaction is increased about 3-fold upon expression of *HHF2/2μ* (Figure 3A and B). In contrast to this, we were unable to detect an interaction of Cse4 Y193A with histone H4. However, expression of *HHF2/2μ* revealed a highly significant increase in the interaction of Cse4 Y193A with histone H4, albeit a lower level than that observed for Cse4-H4 interaction (Figure 3A and B). Taken together, our results show that increased gene dosage of histone H4 facilitates Cse4 Y193A–H4 interaction, and we propose that this contributes to Cse4 Y193A sumoylation, mislocalization, stabilization and SDL phenotype in a *psh1*Δ strain.

Increased gene dosage of histone H4 promotes accumulation of polyubiquitinated Cse4 Y193A in a *cdc48-3* strain under normal physiological conditions

Our results so far have shown a role of histone H4 dosage in the context of overexpressed Cse4 Y193A for its mislocalization. To investigate the physiological consequences of increased gene dosage of histone H4 in a *cse4 Y193A* mutant, we examined the steady state levels of endogenous Cse4 Y193A with and without expression of *HHF2/2μ* in wild-type cells. Steady state levels of endogenous Cse4 Y193A were moderately reduced ($P = 0.0492$), when compared to endogenous wild-type Cse4 (Figure 4A and B). However, expression of *HHF2/2μ* promotes a steady state level of Cse4 Y193A that is comparable to wild-type Cse4 (Figure 4A–C). Subcellular fractionation was done to examine the enrichment of endogenous Cse4 Y193A in chromatin. Similar to the results from *GAL-cse4 Y193A* (Figure 2A), chromatin-associated endogenous Cse4 Y193A was lower when compared to wild-type Cse4 and overexpression of *HHF2* increased chromatin association of Cse4 Y193A even when compared to wild-type Cse4 (Figure 4D and E, and Supplementary Figure S7). These results show that increased gene dosage of histone H4 (*HHF2/2μ*) contributes to higher steady state levels and enrichment of chromatin-association of endogenous Cse4 Y193A.

We have recently reported that endogenous Cse4 at non-centromeric regions is removed by $Cdc48^{Ufd1/Npl4}$ segregase in a Psh1-mediated polyubiquitination-driven manner under normal physiological conditions (35). This study showed that polyubiquitinated endogenous Cse4 in a *cdc48-3* strain is chromatin-associated (35). In agreement with this, soluble pools of endogenous Cse4 are barely detectable compared to endogenous Cse4 in chromatin (Supplementary Figure S7 and (34)). Hence, we investigated whether the polyubiquitination status of endogenous Cse4 Y193A in a *cdc48-3* strain is affected upon increased gene dosage of histone H4. As reported previously, we observed reduced polyubiquitination of Cse4 Y193A in a *cdc48-3* strain (Figure 4F). In contrast, higher levels of polyubiquitinated Cse4 Y193A were observed upon expression of *HHF2/2μ* (Figure 4F and G). Consistent with these results, *cdc48-3 GAL-cse4 Y193A* showed SDL only in strains expressing *HHF2/2μ* (Figure 4H). We conclude that increased gene dosage of histone H4 contributes to increased steady state levels of endogenous Cse4 Y193A, accumulation of polyubiquitinated Cse4 Y193A in chromatin under normal physiological conditions, and SDL phenotype of *cdc48-3 GAL-cse4 Y193A* strain.

Cse4 Y193A is in a 'closed' conformation and increased gene dosage of histone H4 facilitates an 'open' state of Cse4 Y193A

Our results for increased mislocalization of Cse4 Y193A upon increased gene dosage of histone H4 led us to investigate the mechanistic basis for these observations by focusing on the *in vivo* consequences of Cse4–H4 interaction on the conformation of Cse4. A recent study for *in vitro* analysis of Cse4 structure from Malik *et al.* showed that soluble Cse4 exists in a 'closed' conformation due to an interdomain interaction

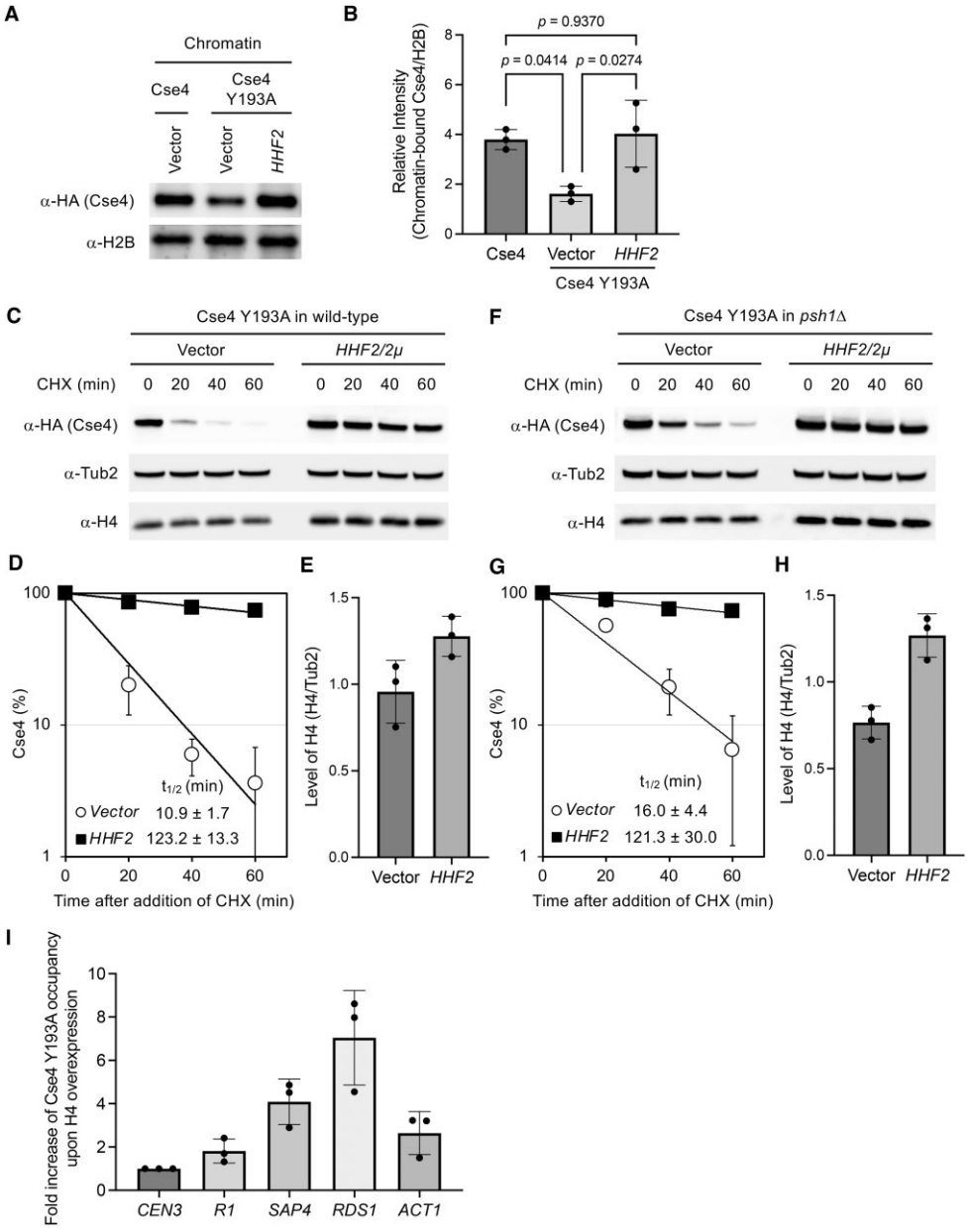

Figure 2. Increased gene dosage of histone H4 contributes to chromatin enrichment, protein stability, and mislocalization of Cse4 Y193A. (**A**) Enrichment of chromatin-associated Cse4 Y193A upon expression of *HHF2/2μ*. Subcellular fractionations were conducted using whole cell extracts prepared from equal numbers of the indicated strains grown in galactose medium for 4 h at 25°C. Cse4 levels in chromatin were monitored by Western blot analysis with anti-HA-antibody. Histone H2B was used as a marker for chromatin fraction. Isogenic yeast strains used here were as follows: wild-type strain (BY4741) transformed with *GAL-CSE4* (pMB1345) or *GAL-cse4 Y193A* (pMB1766) and subsequently transformed with empty vector (pRS425) or *HHF2/2μ* (pMB1929). (**B**) Quantification of levels of chromatin-associated Cse4 Y193A with and without expression of *HHF2/2μ*. Levels of chromatin-associated Cse4 from 2A were quantified in arbitrary density units after normalization to H2B levels. Statistical significance from three biological repeats was assessed by one-way ANOVA (*p*-value = 0.0218) followed by Tukey post-test (all pairwise comparisons of means). Error bars indicate standard deviation from the mean. (**C**) *HHF2/2μ* contributes to increased stability of Cse4 Y193A in a wild-type strain. The indicated strains were grown in galactose medium for 3 hr. Glucose (2%) containing cycloheximide (CHX; 10 μg/ml) was added and cells were collected at the indicated time points. Blots were probed with anti-HA (Cse4), anti-Tub2 (loading control), or anti-H4 antibody. Isogenic yeast strains used here were as follows: wild-type strain (BY4741) transformed with *GAL-cse4 Y193A* (pMB1766) and subsequently transformed with empty vector (pRS425) or *HHF2/2μ* (pMB1929). (**D**) Kinetics of turnover from 2C. Error bars represent standard deviation from the mean of three biological repeats. Cse4 protein half-life ($t_{1/2}$) is indicated as the mean ± SD. The difference in $t_{1/2}$ is statistically significant ($p = 0.0001$). (**E**) Initial levels of histone H4 (0 min) from 2C is indicated. Error bars represent standard deviation from the mean of three biological repeats. (**F**) *HHF2/2μ* contributes to increased stability of Cse4 Y193A in a *psh1*Δ strain. Protein stability assays were performed as described in 2C. Isogenic yeast strains used here were as follows: *psh1*Δ strain (YMB9034) transformed with *GAL-cse4 Y193A* (pMB1766) and subsequently transformed with empty vector (pRS425) or *HHF2/2μ* (pMB1929). (**G**) Kinetics of turnover from 2F. Error bars represent standard deviation from the mean of three biological repeats. Cse4 protein half-life ($t_{1/2}$) is indicated as the mean ± SD. The difference in $t_{1/2}$ is statistically significant ($P = 0.0038$). (**H**) Initial levels of histone H4 (0 min) from 2F is indicated. Error bars represent standard deviation from the mean of three biological repeats. (**I**) Enhanced gene dosage of histone H4 facilitates Cse4 Y193A mislocalization. ChIP-qPCR experiments were performed on chromatin lysates from the indicated strains after growth in galactose medium for 3 h at 25°C. Error bars represent standard deviation from the mean of three biological repeats. Isogenic yeast strains used here were as follows: *psh1*Δ strain (YMB9034) transformed with *GAL-cse4 Y193A* (pMB1766) and subsequently transformed with empty vector (pRS425) or *HHF2/2μ* (pMB1929).

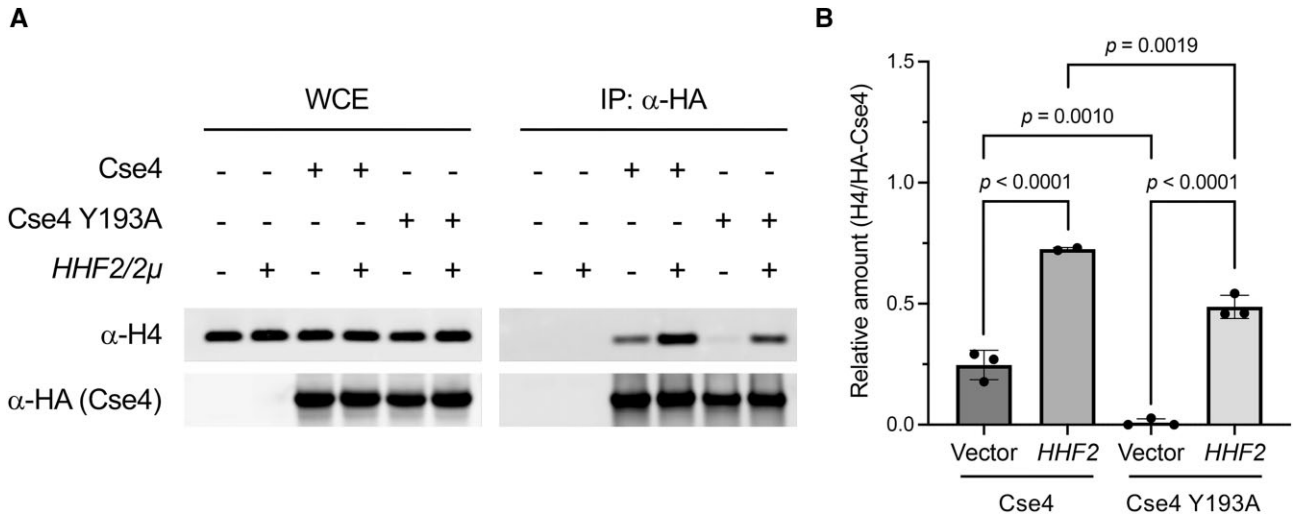

Figure 3. Increased gene dosage of histone H4 facilitates Cse4 Y193A-H4 interaction. (**A**) Cse4 Y193A shows reduced interaction with histone H4, and this is enhanced by expression of *HHF2/2μ*. Protein extracts were prepared from the indicated strains after growth in galactose medium for 3 h at 25°C. Co-IP experiments were performed with anti-HA agarose antibody. Whole cell extracts (WCE) and IP samples were analyzed by Western blot analysis with anti-HA and anti-H4 antibodies. Isogenic yeast strains used here were as follows: wild-type strain (BY4741) transformed with *GAL-CSE4* (pMB1458) or *GAL-cse4 Y193A* (pMB1965) and subsequently transformed with empty vector (pRS425) or *HHF2/2μ* (pMB1929). (**B**) Levels of histone H4 after immunoprecipitation of HA-Cse4 were quantified after normalization to Cse4 levels in the IP (α-HA, IP). Statistical significance from two to three biological repeats was assessed by one-way ANOVA (*P* value < 0.0001) followed by Tukey post-test (all pairwise comparisons of means). Error bars indicate standard deviation from the mean.

between the N-terminal (NTD) and the C-terminal domain (CTD), and binding to histone H4 (obligate partner) enables an 'open' state of Cse4 (44). Atomistic molecular dynamics (MD) simulations for monomeric Cse4 (Movies from (44)) showed that the N-terminus end of Cse4 is located inside the Cse4 structure. In contrast, the N-terminus end of Cse4 is located outside of the Cse4 structure upon the Cse4-H4 complex formation, due to disruption of the interdomain interaction between NTD and CTD. We developed an antibody accessibility (AA) assay that allows us to detect conformational changes of Cse4 between 'open' and 'closed' states *in vivo*. The principle of the AA assay, which was done using N-terminally tagged 8His-HA-Cse4 (Figure 5A), is outlined in Figure 5B. The 'closed' state of N-terminal tagged 8His-HA-Cse4 may not be accessible to anti-HA agarose beads and hence not detected on an anti-HA western blot. However, upon interaction with histone H4, the 'open' state of Cse4 may be accessible to anti-HA agarose beads, thereby giving a signal on a western blot probed with anti-HA antibody (Figure 5B). As a proof of principle, we examined the conformational state of *cse4-102* (L176S M218T) and *cse4-111* (L194Q) mutants, which are defective for Cse4–H4 interaction (48). Consistent with our hypothesis, *cse4-102* and *cse4-111* mutants showed greatly reduced AA (Figures 5C and D), suggesting that the Cse4-102 and Cse4-111 mutant proteins are in a 'closed' form *in vivo*. We confirmed that the His-tagged Cse4-102 and Cse4-111 mutant proteins prepared under the denaturing condition were equally accessible like wild-type Cse4 to Ni-NTA beads (Supplementary Figure S8). It should be noted that sumoylation of Cse4-102 and Cse4-111 is also greatly reduced similar to that observed of Cse4 Y193A sumoylation (43).

We next investigated the conformational state of Cse4 Y193A and structural mimic mutant Cse4 Y193F *in vivo*. In agreement with the reduced interaction of Cse4 Y193A with histone H4 *in vivo* (Figure 3), AA assay showed that wild-type Cse4 is in an 'open' state whereas Cse4 Y193A is predominantly in a 'closed' state (Figures 6A and B). The structurally mimic mutant Cse4 Y193F also exhibits an 'open' state albeit reduced compared to wild-type Cse4 (Figures 6A and B). Consistent with these results, an association of histone H4 was observed for wild-type Cse4 and Cse4 Y193F whereas histone H4 was not detectable due to AA defect in Cse4 Y193A (Supplementary Figure S9). We next asked whether expression of *HHF1/2μ* or *HHF2/2μ* facilitates a conformational change of Cse4 Y193A from 'closed' to 'open' form. Indeed, Cse4 Y193A exhibits an 'open' conformation in strains expressing *HHF1/2μ* or *HHF2/2μ* (Figures 6C and D). Taken together, we conclude that Cse4 Y193A is in a 'closed' conformation and increased gene dosage of histone H4 facilitates a transition to an 'open' state of Cse4 Y193A.

Wild-type histone H4, but not mutant histone H4 (*hhf2-20*), contributes to an 'open' state of Cse4 Y193A and sumoylation

Our model predicts that 'closed' state of Cse4 Y193A is changed to an 'open' state by the interaction of wild-type histone H4 with Cse4 Y193A in strains expressing *HHF1/2μ* or *HHF2/2μ*. If Cse4-H4 interaction is required for the conformational change of Cse4 *in vivo*, we predicted that overexpression of a histone H4 mutant that is defective for Cse4 interaction will not result in a conformational change of Cse4 Y193A. Previous studies have shown that *hhf1-20* with mutations (T82I A89V) in the histone fold domain of histone H4 is defective for interaction with Cse4 (48). Since *HHF1* and *HHF2* are identical proteins, we constructed a *hhf2-20* mutant (Figure 7A). AA assay was done using *GAL-cse4 Y193A* strain expressing vector, *HHF2/2μ*, or *hhf2-20/2μ*. Consistent with our prediction, the AA assay showed an 'open' state of Cse4 Y193A upon expression of *HHF2/2μ*, but not vector or *hhf2-20/2μ* (Figure 7B and C).

We next examined whether the conformational change of Cse4 Y193A to an 'open' state correlates with *GAL-CSE4 psh1*Δ SDL and Cse4 Y193A sumoylation. Growth

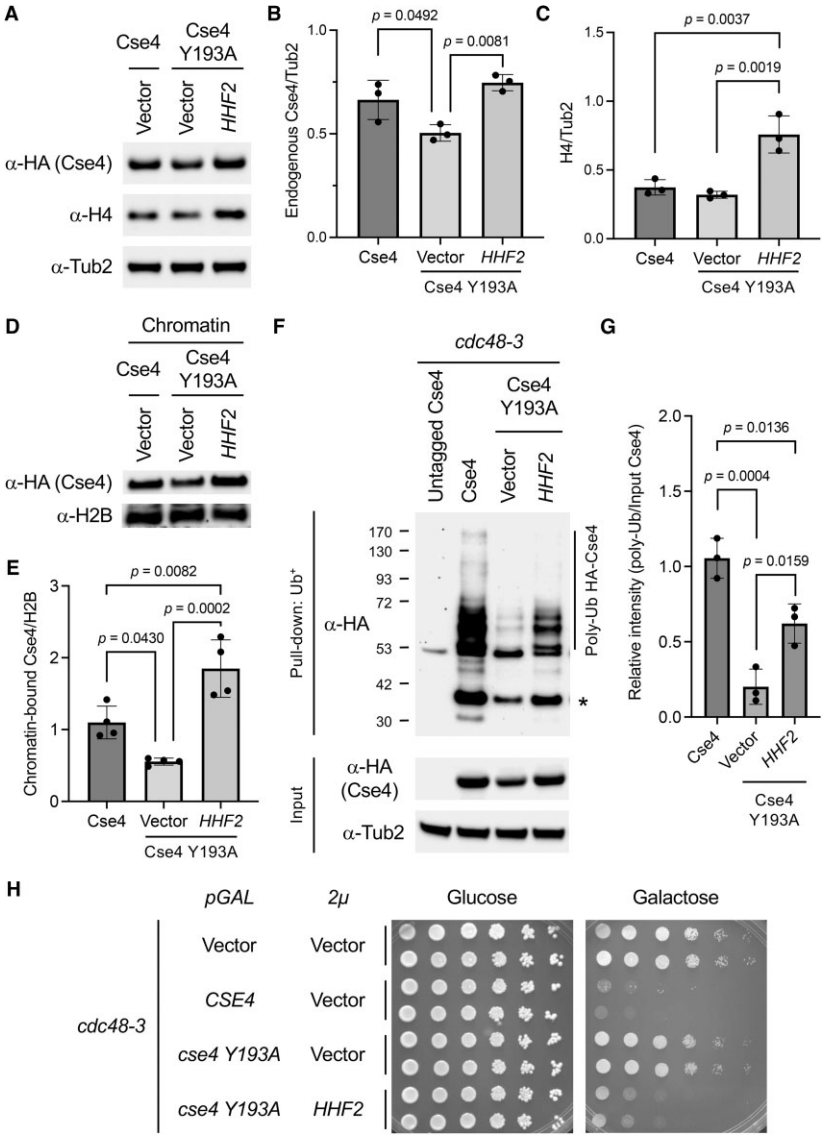

Figure 4. Increased gene dosage of histone H4 contributes to enrichment of Cse4 Y193A in chromatin and accumulation of polyubiquitinated Cse4 Y193A in a *cdc48-3* strain under normal physiological conditions. (**A**) Increased steady state levels of endogenous Cse4 Y193A upon expression of *HHF2/2μ*. The indicated strains were grown to logarithmic phase in glucose (2%)-containing synthetic medium selective for the plasmids. Protein extracts were analyzed by Western blot analysis with anti-HA (Cse4), anti-H4 or anti-Tub2 (loading control) antibody. Isogenic yeast strains used here were as follows: wild-type (YMB11160) or *cse4 Y193A* mutant (YMB11163) cells transformed with empty vector (pRS425) or *HHF2/2μ* (pMB1929). (**B**) Levels of endogenous Cse4 from 4A were quantified in arbitrary density units after normalization to Tub2 levels. Statistical significance from three biological repeats was assessed by one-way ANOVA (*p*-value = 0.0092) followed by Tukey post-test (all pairwise comparisons of means). Error bars indicate standard deviation from the mean. (**C**) Levels of histone H4 from 4A were quantified in arbitrary density units after normalization to Tub2 levels. Statistical significance from three biological repeats was assessed by one-way ANOVA (*p*-value = 0.0015) followed by Tukey post-test (all pairwise comparisons of means). Error bars indicate standard deviation from the mean. (**D**) Increased levels of chromatin-associated endogenous Cse4 Y193A upon expression of *HHF2/2μ*. Subcellular fractionations were conducted using whole cell extracts prepared from equal numbers of logarithmically growing cells in glucose (2%)-containing synthetic medium selective for the plasmids. Cse4 levels in chromatin were monitored by Western blot analysis with anti-HA-antibody. Histone H2B was used as markers for chromatin fraction. Isogenic yeast strains used here were as follows: wild-type (YMB11160) or *cse4 Y193A* mutant (YMB11163) cells transformed with empty vector (pRS425) or *HHF2/2μ* (pMB1929). (**E**) Levels of chromatin-associated endogenous Cse4 from 4D were quantified in arbitrary density units after normalization to H2B levels. Statistical significance from four biological repeats was assessed by one-way ANOVA (*p*-value = 0.0003) followed by Tukey post-test (all pairwise comparisons of means). Error bars indicate standard deviation from the mean. (**F**) Increased gene dosage of histone H4 contributes to accumulation of polyubiquitinated endogenous Cse4 Y193A in a *cdc48-3* strain. Ub pull-down assay was performed using protein extracts from logarithmically growing cells in glucose (2%)-containing synthetic medium selective for the plasmids. Input and ubiquitin pull-down samples were analyzed using anti-HA (Cse4) and anti-Tub2 antibodies. Untagged Cse4 was used as a negative control. Asterisk shows nonmodified Cse4. Isogenic yeast strains used here were as follows: *cdc48-3 6His-3HA-CSE4::NatR* (YMB10652) or *cdc48-3 6His-3HA-cse4 Y193A::NatR* (YMB11619) strain transformed with empty vector (pRS425) or *HHF2/2μ* (pMB1929). (**G**) Levels of polyubiquitinated Cse4 from 4F were quantified in arbitrary density units after normalization to input Cse4. Statistical significance from three biological repeats was assessed by one-way ANOVA (*P*-value = 0.0005) followed by Tukey post-test (all pairwise comparisons of means). Error bars indicate standard deviation from the mean. (**H**) *GAL-cse4 Y193A cdc48-3* strain exhibits SDL with *HHF2/2μ*. Cells were spotted in five-fold serial dilutions on glucose (2%)- or galactose (2%)-containing synthetic medium selective for the plasmids. The plates were incubated at 25°C for 4 days. Isogenic yeast strains used here were as follows: *cdc48-3* strain (PK1658) transformed with *GAL-CSE4* (pMB1345) or *GAL-cse4 Y193A* (pMB1766) and subsequently transformed with empty vector (pRS425) or *HHF2/2μ* (pMB1929).

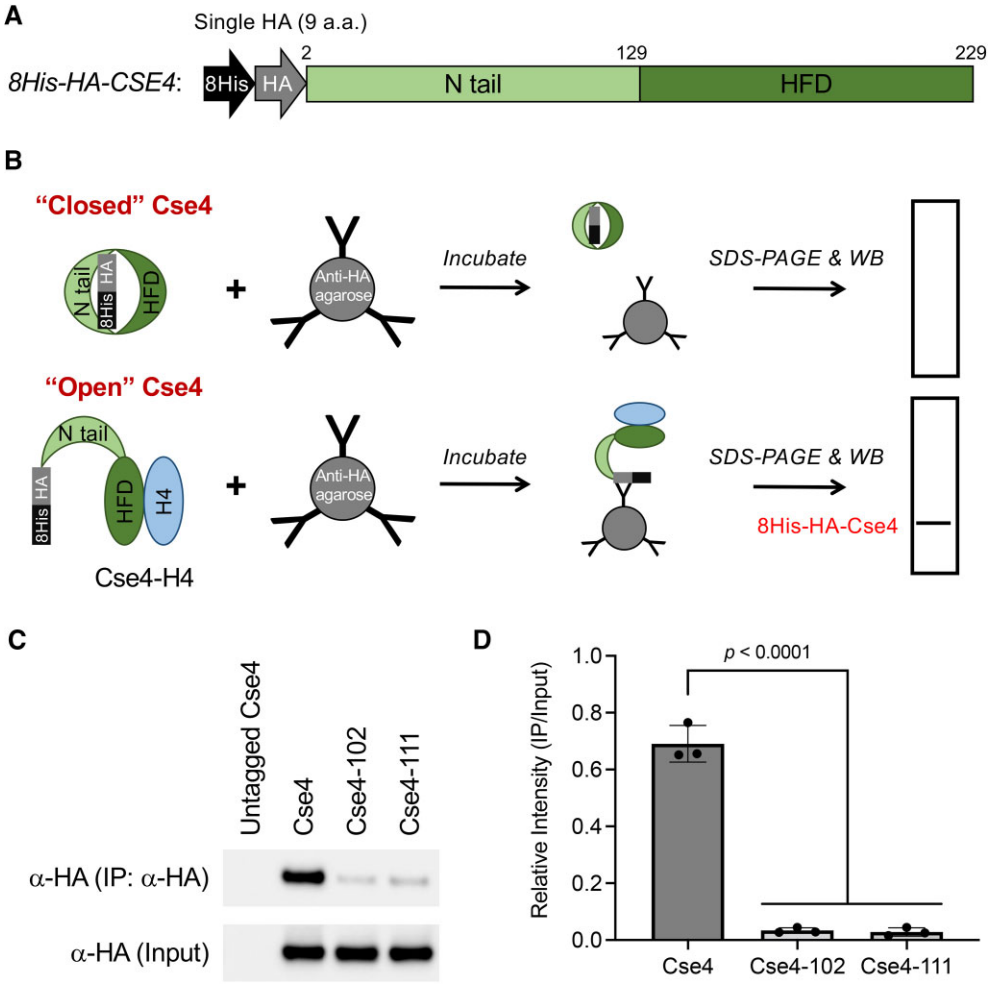

Figure 5. Antibody Accessibility (AA) assay for conformational state of Cse4 *in vivo*. (**A**) Schematic showing N-terminally tagged 8His-HA-Cse4. N-terminal tail and histone hold domain (HFD) are pale and dark greens, respectively. (**B**) AA assay can detect 'open' but not 'closed' form of Cse4. The 'closed' form of N-terminally tagged 8His-HA-Cse4 will not be accessible to anti-HA agarose beads and hence not detected on anti-HA western blot. The "open' form will be accessible to anti-HA agarose beads giving a signal on the anti-HA western blot. (**C**) The Cse4-H4 dimer defective mutants, Cse4-102 and Cse4-111, showed reduced AA and 'closed' form. AA assay was performed using the indicated strains after transient induction of Cse4 in galactose medium for 4 h at 25°C. Input and IP (α-HA, IP) samples were resolved by SDS-PAGE and levels of Cse4 were monitored by Western blot analysis with anti-HA-antibody. Isogenic yeast strains used here were as follows: wild-type strain (BY4741) transformed with *GAL-CSE4* (pMB1345), *GAL-cse4-102* (pMB1984), or *GAL-cse4-111* (pMB1988). (**D**) Levels of Cse4 that bind to anti-HA agarose beads from 5C were quantified in arbitrary density units after normalization to input levels. Statistical significance from three biological repeats was assessed by one-way ANOVA (*P*-value < 0.0001) followed by Tukey post-test (all pairwise comparisons of means). Error bars indicate standard deviation from the mean.

assay showed that *HHF2/2μ*, but not *hhf2-20/2μ*, exhibits SDL in a *psh1Δ GAL-cse4 Y193A* strain (Figure 7D and Supplementary Figure S10). Sumoylation assay showed that *HHF2/2μ*, but not *hhf2-20/2μ*, increased the sumoylation of Cse4 Y193A (Figure 7E and F). These results show that an 'open' conformation of Cse4 Y193A correlates with its sumoylation and SDL of *psh1Δ GAL-cse4 Y193A* strain.

Accumulation of polyubiquitinated endogenous Cse4 Y193A in a *cdc48-3* strain is specific to *HHF2,* but not *hhf2-20* or *hhf2 R36A*

The correlation of 'open' and 'closed' states of Cse4 Y193A in strains with and without *HHF2/2μ*, respectively, led us to examine how this affects the accumulation of polyubiquitinated endogenous Cse4 Y193A in a *cdc48-3* strains. Growth assays showed that *cdc48-3 GAL-cse4 Y193A* with *HHF2/2μ*, but not *hhf2-20/2μ*, exhibits SDL on galactose plate (Figure 8A) similar to results for *psh1Δ cse4 Y193A* strain (Figure 7D and Supplementary Figure S10). Growth similarities between *psh1Δ* and *cdc48-3* background support our previous studies that Psh1-mediated polyubiquitination of Cse4 is subsequently recognized by $Cdc48^{Ufd1/Npl4}$ segregase for removal from chromatin (35). We observed the accumulation of polyubiquitinated Cse4 Y193A in a *cdc48-3* strain expressing *HHF2/2μ*, but not in *cdc48-3* strain with *hhf2-20/2μ* (Figure 8B and C). These results show that increased gene dosage of histone H4 facilitates an 'open' conformation of Cse4 Y193A with accumulation in a polyubiquitinated state in a *cdc48-3* strain.

We next examined the relevance of histone H4 in the interaction of Cse4 with Psh1 and the accumulation of polyubiquitinated Cse4 in a *cdc48-3* strain. The rationale for this is based on results from Deyter *et al.* showing that mutation of histone H4 R36 exhibits reduced interaction between Cse4 and Psh1 (49). Since Psh1 contributes to polyubiquitination of

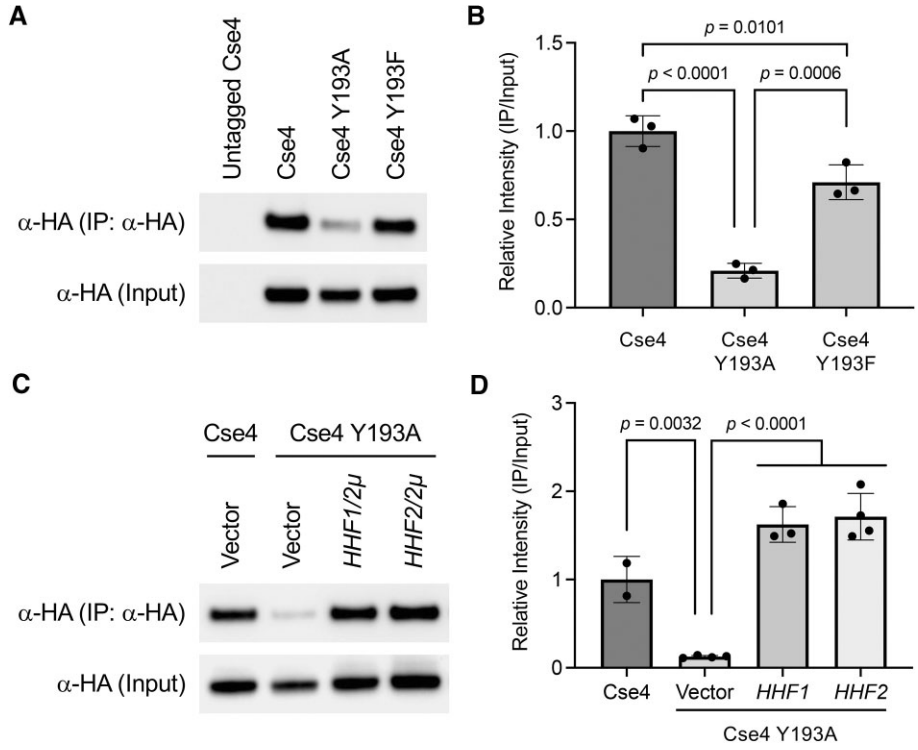

Figure 6. Cse4 Y193A is in a 'closed' configuration and increased gene dosage of histone H4 facilitates an 'open' state of Cse4 Y193A. (**A**) Cse4 Y193A showed reduced AA and is in a 'closed' state. AA assay was performed using the indicated strains after growth of strains in galactose medium for 4 h at 25°C. Input and IP (α-HA, IP) samples were resolved by SDS-PAGE and levels of Cse4 were monitored by Western blot analysis with anti-HA-antibody. Isogenic yeast strains used here were as follows: wild-type strain (BY4741) transformed with *GAL-CSE4* (pMB1345), *GAL-cse4 Y193A* (pMB1766), or *GAL-cse4 Y193F* (pMB1787). (**B**) Quantification of the relative levels of Cse4 that binds to anti-HA agarose beads after normalization to input levels. Statistical significance from three biological repeats was assessed by one-way ANOVA (*P*-value < 0.0001) followed by Tukey post-test (all pairwise comparisons of means). Error bars indicate standard deviation from the mean. (**C**) Enhanced gene dosage of histone H4 promotes AA and an 'open' form of Cse4 Y193A. AA assays were conducted as describe in 6A. Isogenic yeast strains used here were as follows: wild-type strain (BY4741) transformed with *GAL-CSE4* (pMB1345) or *GAL-cse4 Y193A* (pMB1766) and subsequently transformed with empty vector, *HHF1/2μ* (pMB1928), or *HHF2/2μ* (pMB1929). (**D**) Quantification of the relative levels of Cse4 that bind to anti-HA agarose beads after normalization to input levels. Statistical significance from multiple experiments was assessed by one-way ANOVA (*p*-value < 0.0001) followed by Tukey post-test (all pairwise comparisons of means). Error bars indicate standard deviation from the mean.

endogenous chromatin-associated Cse4 in a *cdc48-3* strain, we asked whether histone H4 R36A mutation shows reduced levels of polyubiquitinated Cse4 Y193A in a *cdc48-3* strain due to defects of the Cse4-Psh1 interaction. Indeed, the accumulation of polyubiquitinated Cse4 Y193A in a *cdc48-3* strain was greatly reduced upon expression of *hhf2 R36A/2μ* (Figure 8B and C). In contrast to *cse4 Y193A hhf2-20* strain, *cse4 Y193A hhf2 R36A* strain exhibits SDL on galactose plate (Figure 8A) due to the 'open' form of Cse4 Y193A (Figure 8D and E). These findings support the specific role of histone H4 R36 as a key residue promoting the Cse4-Psh1 interaction that is independent of Cse4 mislocalization. Taken together, we conclude that an 'open' state of Cse4 Y193A upon expression of *HHF2/2μ* leads to accumulation of polyubiquitinated Cse4 Y193A in a *cdc48-3* strain.

Histone H4 gene dosage regulates the conformational state of wild-type Cse4

Our results showing that increased gene dosage of histone H4 contributes to an 'open' state of Cse4 Y193A prompted us to examine whether histone H4 gene dosage affects the conformational state of wild-type Cse4 *in vivo*. We performed AA assay using strains deleted for either one of the histone H4 alleles (*hhf1*Δ and *hhf2*Δ). Wild-type Cse4 predominantly exhibits a 'closed' state in *hhf1*Δ and *hhf2*Δ strains (Figure 9A and B). Consistent with a correlation between the sumoylation and 'open' state of Cse4, we have previously reported that Cse4 sumoylation is defective in *hhf1*Δ and *hhf2*Δ strains (43). Taken together, we conclude that Cse4–H4 interaction facilitates an 'open' state of wild-type Cse4 for its sumoylation.

Discussion

The incorporation of CENP-A into centromeric chromatin is essential for establishing centromere identity and preventing CIN. Mislocalization of overexpressed CENP-A to non-centromeric chromatin contributes to CIN in yeasts, flies, and humans (13–19). Overexpression and mislocalization of CENP-A are observed in many cancers and this correlates with poor prognosis. In this study, we investigated how the *in vivo* conformation of Cse4 affects the localization of Cse4 to non-centromeric regions. Our results show that increased gene dosage of histone H4 facilitates *in vivo* conformational change of Cse4 that contributes to Cse4 sumoylation and mislocalization. We propose a model in which monomer Cse4 is in a 'closed' state and interaction of Cse4 with histone H4 alters the conformation of Cse4 to an 'open' state *in vivo* (Figure 9C). The 'open' state of Cse4 correlates with its

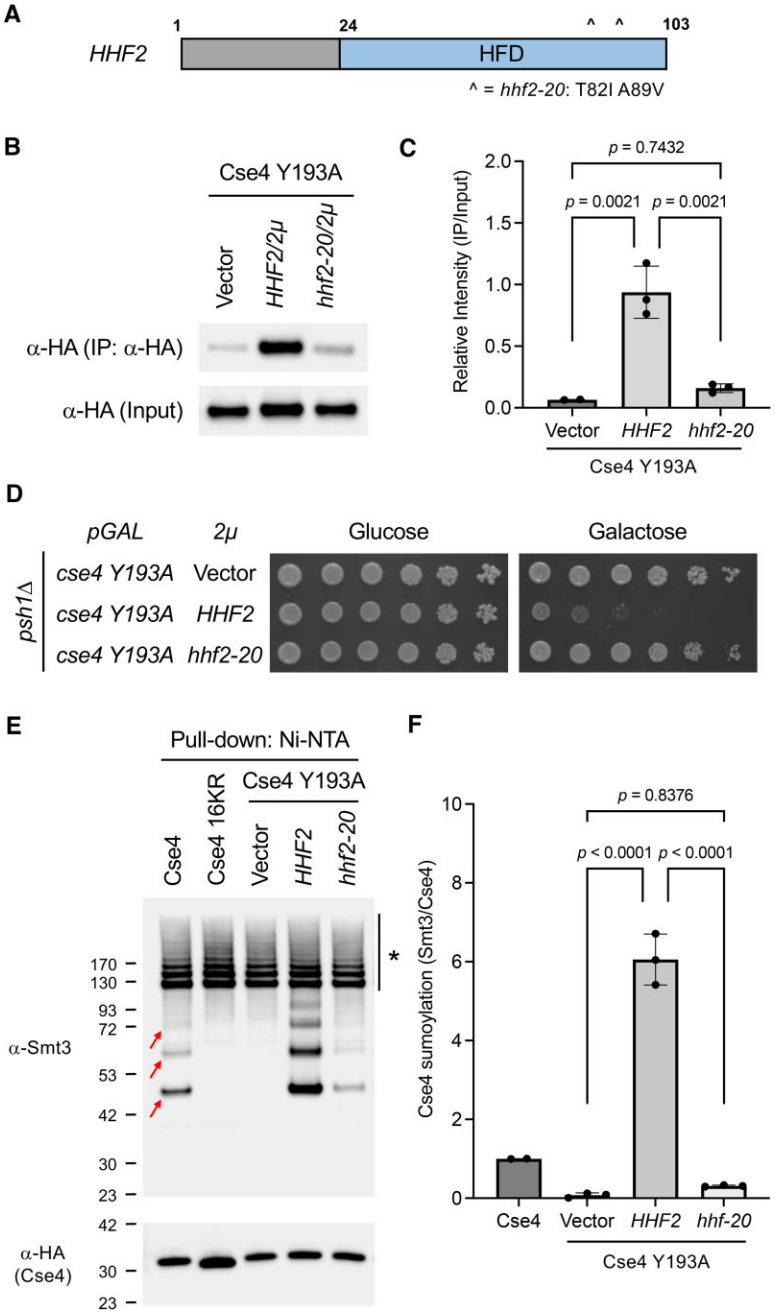

Figure 7. Wild-type histone H4, but not mutant Hhf2-20, contributes to an 'open' conformation of Cse4 Y193A. (**A**) Schematic of *hhf2-20* (T82I A89V) mutant. HFD: histone fold domain. (**B**) AA of Cse4 Y193A due to 'open' state in strains expressing *HHF2/2μ* but not the Cse4-H4 dimer defective mutant *hhf2-20/2μ*. AA assay was performed using the indicated strains after transient induction of Cse4 in galactose medium for 4 h at 25°C. Input and IP (α-HA, IP) samples were resolved by SDS-PAGE and levels of Cse4 were monitored by Western blot analysis with anti-HA-antibody. Isogenic yeast strains used here were as follows: wild-type strain (BY4741) transformed with *GAL-cse4 Y193A* (pMB1766) and subsequently transformed with empty vector (pRS425), *HHF2/2μ* (pMB1929), or *hhf2-20/2μ* (pMB2061). (**C**) Quantification of the relative levels of Cse4 that bind to anti-HA agarose beads after normalization to input levels. Statistical significance from two to three biological repeats was assessed by one-way ANOVA (p-value = 0.0012) followed by Tukey post-test (all pairwise comparisons of means). Error bars indicate standard deviation from the mean. (**D**) SDL phenotype of *GAL-cse4 Y193A psh1*Δ strain observed upon expression of *HHF2/2μ* but not the Cse4-H4 dimer defective mutant *hhf2-20/2μ*. Growth assays were performed by plating five-fold serial dilution of cells on glucose (2%)- or galactose (2%)-containing synthetic medium selective for the plasmids. The plates were incubated at 25°C for 4 days. Isogenic yeast strains used here were as follows: *psh1*Δ strain (YMB9034) transformed with *GAL-cse4 Y193A* (pMB1766) and subsequently transformed with empty vector (pRS425), *HHF2/2μ* (pMB1929), or *hhf2-20/2μ* (pMB2061). (**E**) Increased sumoylation of Cse4 Y193A upon expression of *HHF2/2μ* but not the Cse4-H4 dimer defective mutant *hhf2-20/2μ*. Levels of sumoylated Cse4 were assayed from the indicated strains after growth in galactose medium for 4 h at 25°C. Arrows indicate the three high molecular weight bands that represent sumoylated Cse4. Cse4 16KR, in which all 16 lysine (K) residues are mutated to arginine (R), is used as a negative control. Asterisk indicates nonspecific sumoylated proteins that bind to beads. Isogenic yeast strains used here were as follows: wild-type strain (BY4741) transformed with *GAL-CSE4* (pMB1345), *GAL-cse4 16KR* (pMB1344), or *GAL-cse4 Y193A* (pMB1766) and subsequently transformed with empty vector (pRS425), *HHF2/2μ* (pMB1929), or *hhf2-20/2μ* (pMB2061). (**F**) Quantification of the relative levels of sumoylated Cse4. Levels of sumoylated Cse4 were normalized to nonmodified Cse4 probed against HA in the pull-down samples. Statistical significance from two to three biological repeats was assessed by one-way ANOVA (p-value < 0.0001) followed by Tukey post-test (all pairwise comparisons of means). Error bars indicate standard deviation from the mean.

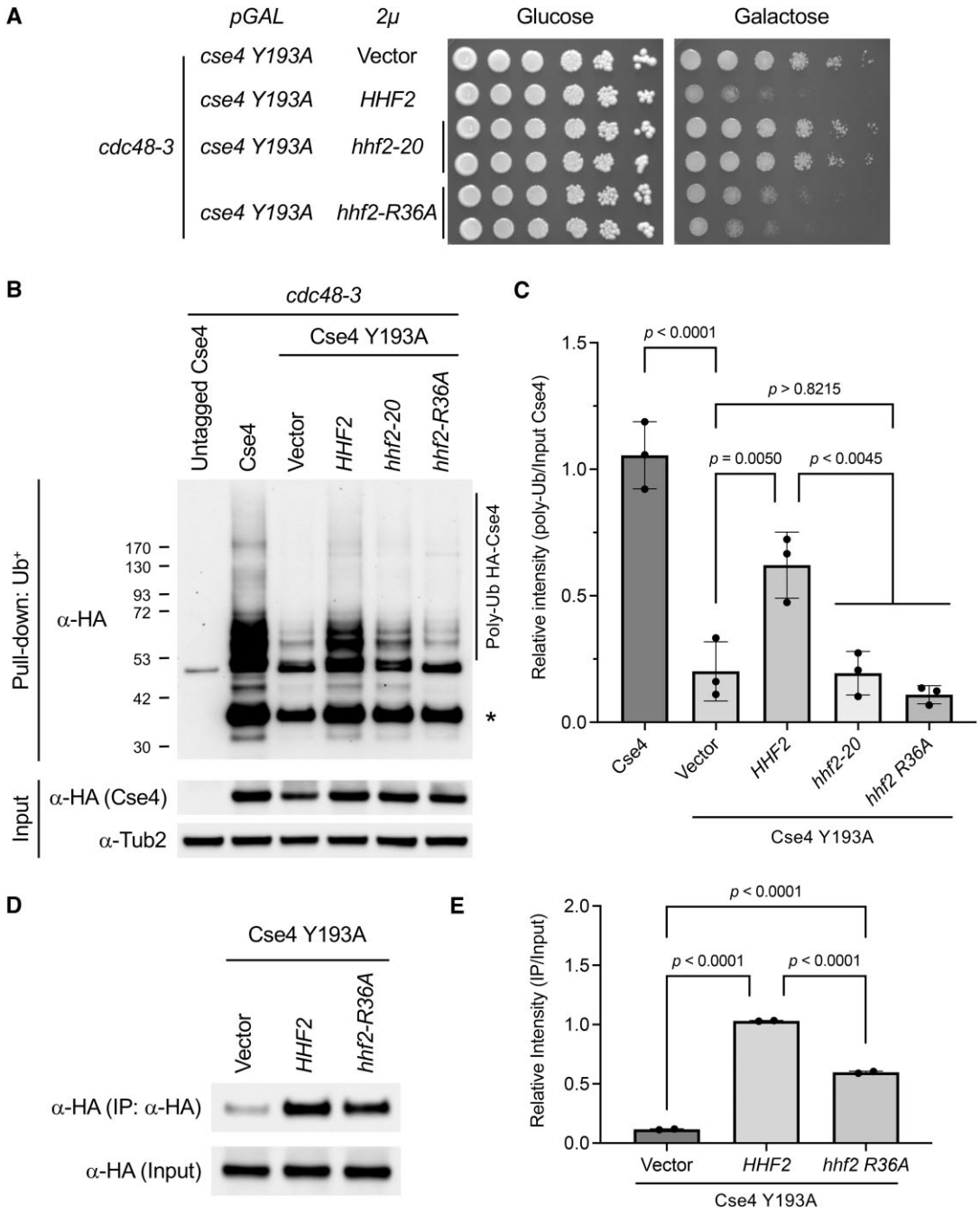

Figure 8. Strains expressing *HHF2/2μ*, but not *hhf2-20* and *hhf2 R36A*, show accumulation of polyubiquitinated endogenous Cse4 Y193A. (**A**) *GAL-cse4 Y193A* with *HHF2/2μ* or *hhf2 R36A/2μ* lead to SDL in a *cdc48-3* strain. Growth assays were performed by plating five-fold serial dilution of cells on glucose (2%)- or galactose (2%)-containing synthetic medium selective for the plasmids. The plates were incubated at 25°C for 5 days. Isogenic yeast strains used here were as follows: *cdc48-3* strain (PK1658) transformed with *GAL-cse4 Y193A* (pMB1766) and subsequently transformed with empty vector (pRS425), *HHF2/2μ* (pMB1929), *hhf2-20/2μ* (pMB2061), or *hhf2 R36A/2μ* (pMB2063). (**B**) Reduced accumulation of polyubiquitinated Cse4 Y193A in strains expressing *hhf2-20/2μ* and *hhf2 R36A/2μ* in a *cdc48-3* strain. Ub pull-down assay was performed using protein extracts from logarithmically growing cells in glucose (2%)-containing synthetic medium selective for the plasmids. Input and ubiquitin pull-down samples were analyzed using anti-HA (Cse4) and anti-Tub2 antibodies. Untagged Cse4 was used as a negative control. Asterisk shows nonmodified Cse4. Isogenic yeast strains used here were as follows: *cdc48-3 6His-3HA-CSE4::NatR* (YMB10652) or *cdc48-3 6His-3HA-cse4 Y193A::NatR* (YMB11619) strain transformed with empty vector (pRS425), *HHF2/2μ* (pMB1929), *hhf2-20/2μ* (pMB2061), or *hhf2 R36A/2μ* (pMB2063). (**C**) Levels of polyubiquitinated Cse4 from 8B were quantified in arbitrary density units after normalization to input Cse4. Statistical significance from three biological repeats was assessed by one-way ANOVA (*P*-value < 0.0001) followed by Tukey post-test (all pairwise comparisons of means). Error bars indicate standard deviation from the mean. (**D**) Cse4 Y193A exhibits an 'open' conformation upon expression of *hhf2 R36A*. AA assay was performed using the indicated strains after growth in galactose medium for 4 h at 25°C. Input and IP (α-HA, IP) samples were resolved by SDS-PAGE and levels of Cse4 were monitored by Western blot analysis with anti-HA-antibody. Isogenic yeast strains used here were as follows: wild-type strain (BY4741) transformed with *GAL-cse4 Y193A* (pMB1766) and subsequently transformed with empty vector (pRS425), *HHF2/2μ* (pMB1929) or *hhf2 R36A/2μ* (pMB2063). (**E**) Levels of Cse4 that bind to anti-HA agarose beads from 8D were quantified in arbitrary density units after normalization to input levels. Statistical significance from two biological repeats was assessed by one-way ANOVA (*P*-value < 0.0001) followed by Tukey post-test (all pairwise comparisons of means). Error bars indicate standard deviation from the mean.

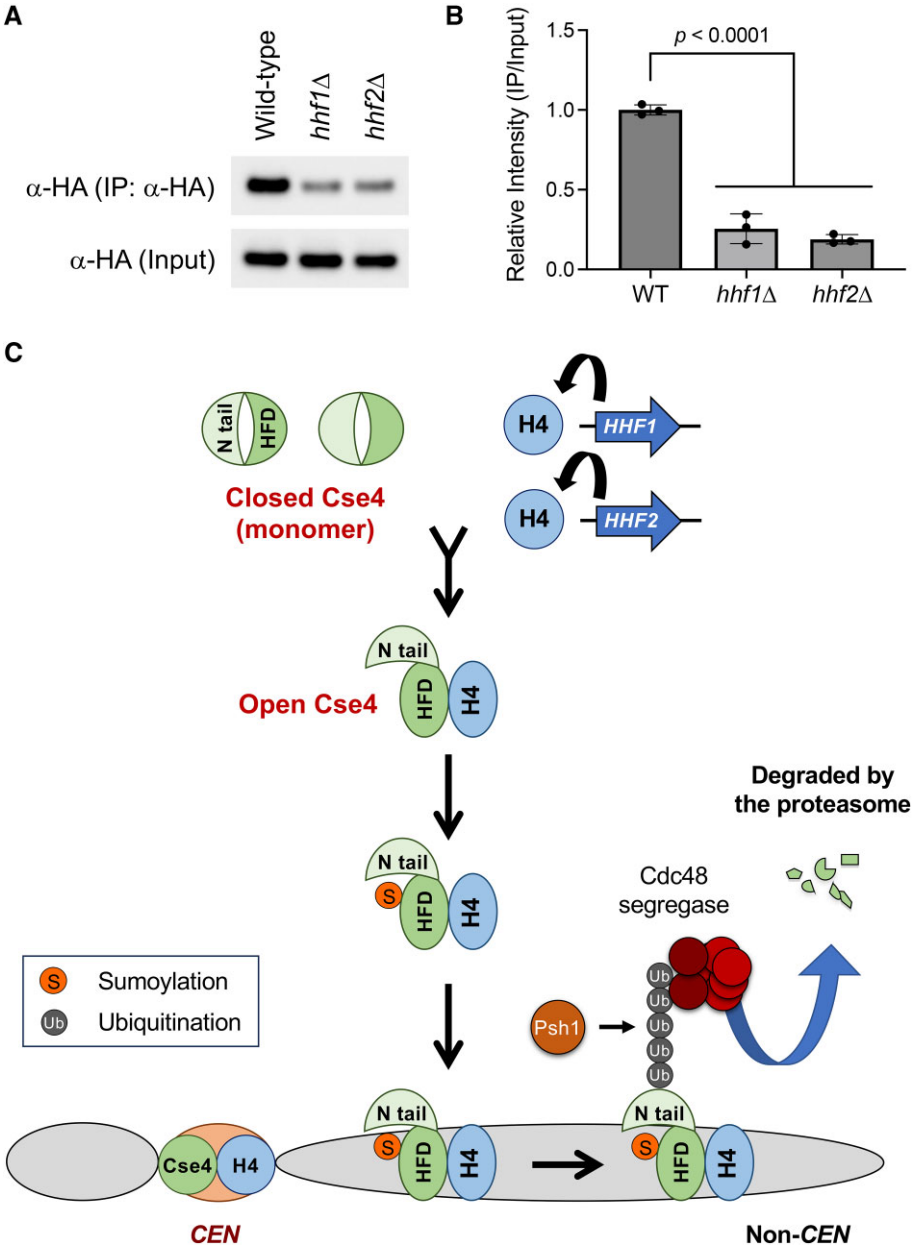

Figure 9. Histone H4 gene dosage regulates the conformational state of wild-type Cse4. (**A**) Wild-type Cse4 predominantly exhibits a 'closed' state in *hhf1*Δ and *hhf2*Δ strains. AA assay was performed using the indicated strains after growth in galactose medium for 4 h at 25°C. Input and IP (α-HA, IP) samples were resolved by SDS-PAGE and levels of Cse4 were monitored by Western blot analysis with anti-HA-antibody. Isogenic yeast strains used here were as follows: wild-type (BY4741), *hhf1*Δ (YMB10766), and *hhf2*Δ (YMB10767) strains transformed with *GAL-CSE4* (pMB1345). (**B**) Quantification of the relative levels of Cse4 that bind to anti-HA agarose beads after normalization to input levels. Statistical significance from three biological repeats was assessed by one-way ANOVA (*P*-value < 0.0001) followed by Tukey post-test (all pairwise comparisons of means). Error bars indicate standard deviation from the mean. (**C**) Interaction of histone H4 with Cse4 facilitates conformational changes in Cse4 for its sumoylation and mislocalization. Model depicts a proposal of how Cse4–H4 interaction promotes conformational change in Cse4 for its mislocalization. Monomer Cse4 is in a 'closed' state *in vivo* and interaction of Cse4 with histone H4 contributes to a change in the conformation of Cse4 to an 'open' state. The 'open' state of Cse4 facilitates its sumoylation and mislocalization to non-centromeric regions. Mislocalized Cse4, which is in an 'open" state, is polyubiquitinated by Psh1, and this promotes the interaction between polyubiquitinated Cse4 and the $Cdc48^{Ufd1/Npl4}$ segregase complex, resulting in the removal of Cse4 from non-centromeric regions for proteasomal degradation (35).

sumoylation, protein stability, enrichment in chromatin, mislocalization to non-centromeric regions, SDL phenotype in *psh1*Δ and *cdc48-3* strains, and accumulation of polyubiquitinated form of Cse4 in a *cdc48-3* strain under normal physiological conditions. Our results provide the first evidence that Cse4-H4 interaction contributes to an 'open' conformation of Cse4 *in vivo*, thereby facilitating sumoylation and mislocalization of Cse4.

We used Cse4 Y193A as a tool to examine molecular events that contribute to the mislocalization of Cse4 *in vivo*. Cse4 Y193A with all 16 lysine residues intact is ideally suited for this study because unlike *cse4-102* and *cse4-111*, which are defective for centromere function (48), Cse4 Y193A only exhibits defects in non-centromeric localization while centromeric deposition is unaffected. Overexpressed Cse4 Y193A does not exhibit SDL in *psh1Δ* and *cdc48-3* strains due to re-

duced mislocalization. Increased gene dosage of histone H4 contributes to increased sumoylation, protein stability, mislocalization of Cse4 Y193A in a wild-type strain and accumulation of polyubiquitinated Cse4 Y193A in a *cdc48-3* strain. Consistent with these results, Co-IP experiments showed that Cse4 Y193A exhibits reduced interaction with histone H4, and increased gene dosage of histone H4 promotes Cse4 Y193A-H4 interaction. In addition, increased gene dosage of histone H4 promotes increased Cse4-H4 interaction and *GAL-CSE4* SDL phenotype in a wild-type strain. Several studies have highlighted the importance of maintaining proper histone gene dosage for preventing CIN. For example, stoichiometric balance of canonical histone pairs (H2A-H2B or H3-H4) is essential for high fidelity of mitotic chromosome transmission in budding yeast (15). Strains with reduced gene dosage of histone H4 (*hhf1*Δ or *hhf2*Δ) exhibit defects in Cse4 sumoylation, reduced mislocalization of Cse4, and lack of SDL in a *psh1*Δ *GAL-CSE4* strain (43). Constitutive expression of histone H3 due to a partial deletion of the promoter of H3 (*Δ16H3*) suppresses the mislocalization of Cse4 K16R and the chromosome loss phenotype in *GAL-cse4 K16R* strains (15). Moreover, increased gene dosage of histone H3 and H4, which restores balance of H3-H4 stoichiometry, showed a lack of SDL in a *psh1*Δ *GAL-cse4 Y193A* strain (Supplementary Figure S11). Thus, increased gene dosage of histone H4, which promotes Cse4-H4 interaction, leads to Cse4 mislocalization.

In this study, we developed a new *in vivo* approach, Antibody Accessibility (AA) assay, to examine and define the molecular mechanism by which conformational changes of Cse4 between 'open' and 'closed' states contribute to Cse4 mislocalization. The AA assay is a simple and powerful tool to detect potential and otherwise hidden protein structural changes *in vivo* that can also be used to study other proteins. The interaction of Cse4 with histone H4 facilitates an 'open' state of Cse4 which is critical for Cse4 sumoylation and mislocalization, as well as *GAL-CSE4* SDL in *psh1Δ* and *cdc48-3* strains. The AA assay showed reduced accessibility of Cse4 Y193A with anti-HA-antibody *in vivo* suggesting that Cse4 Y193A is predominantly in a 'closed' conformation. Increased gene dosage of histone H4 facilitated a conformational change of Cse4 Y193A to an 'open' state. Expression of Cse4-H4 dimer defective mutant *hhf2-20/2μ* did not change the 'closed' state of Cse4 Y193A to 'open', suggesting that a functional interaction of histone H4 is required for a conformational change in Cse4 Y193A *in vivo*. Notably, our *in vitro* binding studies showed that both wild-type Cse4 and Cse4 Y193A interact with histone H4 and dissociate from histone H4 in a similar manner (Supplementary Figure S12). Since we observed reduced interaction between Cse4 Y193A and histone H4 *in vivo*, we propose that in addition to histone H4, other factors such as histone chaperones may also contribute to the *in vivo* conformation of Cse4 upon interaction with histone H4. Future studies will allow us to identify proteins that regulate *in vivo* conformation of Cse4 and how these contribute to Cse4 mislocalization.

We observed reduced sumoylation and polyubiquitination of Cse4 Y193A, supporting the idea that the 'closed' form of Cse4 has limited access to SUMO and ubiquitin modifying enzymes *in vivo*. Open state of Cse4 Y193A upon increased gene dosage of histone H4 enable to access to those E3 ligases. H4 R36 is a key residue that promotes Cse4 interaction with E3 ubiquitin ligase Psh1 (49). Open state of Cse4 Y193A upon increased gene dosage of *hhf2 R36A* is consistent with the SDL of *cdc48-3 GAL-cse4 Y193A hhf2 R36A* strain, suggesting that chromatin-associated mislocalized Cse4 is in an 'open' state.

In summary, we have established that *in vivo* conformational changes of Cse4 regulates its sumoylation and mislocalization to non-centromeric regions. We propose that monomer Cse4 Y193A is in a 'closed' form *in vivo*. Increased gene dosage of histone H4 facilitates the formation of a Cse4 Y193A-H4 dimer, and to an 'open' state of Cse4 Y193A. Interestingly, human CENP-A has F101, instead of Y (35). Structurally mimetic mutant Cse4 Y193F is in an 'open' state similar to wild-type Cse4. Based on the conservation between Cse4 Y193 and CENP-A F101, it is of interest to examine the role of CENP-A F101 in localization of CENP-A to centromeric and non-centromeric regions in human cells. These studies will elucidate mechanisms that contribute to mislocalization of CENP-A in human cancers.

Data availability

All experimental data sets are available at Figshare (https://doi.org/10.6084/m9.figshare.24435463).

Supplementary data

Supplementary Data are available at NAR Online.

Acknowledgements

We gratefully acknowledge Ashutosh Kumar, Santanu K. Ghosh and Shivangi Shukla for valuable discussions. We thank David J. Clark for *HHT1-HHF1/2μ* plasmid and the members of the Basrai laboratory for helpful discussions and comments on the manuscript.

Funding

National Institutes of Health Intramural Research Program at the National Cancer Institute (to M.A.B.); National Institutes of Health [R35GM148350 to P.K.]. Funding for open access charge: National Institutes of Health Intramural Research Program.

Conflict of interest statement

None declared.

References

1. Torras-Llort,M., Moreno-Moreno,O. and Azorin,F. (2009) Focus on the centre: the role of chromatin on the regulation of centromere identity and function. *EMBO J.*, **28**, 2337–2348.
2. Biggins,S. (2013) The composition, functions, and regulation of the budding yeast kinetochore. *Genetics*, **194**, 817–846.
3. McKinley,K.L. and Cheeseman,I.M. (2016) The molecular basis for centromere identity and function. *Nat. Rev. Mol. Cell Biol.*, **17**, 16–29.
4. Camahort,R., Li,B., Florens,L., Swanson,S.K., Washburn,M.P. and Gerton,J.L. (2007) Scm3 is essential to recruit the histone H3 variant Cse4 to centromeres and to maintain a functional kinetochore. *Mol. Cell*, **26**, 853–865.

5. Mizuguchi,G., Xiao,H., Wisniewski,J., Smith,M.M. and Wu,C. (2007) Nonhistone Scm3 and histones CenH3-H4 assemble the core of centromere-specific nucleosomes. *Cell*, **129**, 1153–1164.
6. Stoler,S., Rogers,K., Weitze,S., Morey,L., Fitzgerald-Hayes,M. and Baker,R.E. (2007) Scm3, an essential Saccharomyces cerevisiae centromere protein required for G2/M progression and Cse4 localization. *Proc. Natl. Acad. Sci. U.S.A.*, **104**, 10571–10576.
7. Williams,J.S., Hayashi,T., Yanagida,M. and Russell,P. (2009) Fission yeast Scm3 mediates stable assembly of Cnp1/CENP-A into centromeric chromatin. *Mol. Cell*, **33**, 287–298.
8. Pidoux,A.L., Choi,E.S., Abbott,J.K., Liu,X., Kagansky,A., Castillo,A.G., Hamilton,G.L., Richardson,W., Rappsilber,J., He,X., *et al.* (2009) Fission yeast Scm3: a CENP-A receptor required for integrity of subkinetochore chromatin. *Mol. Cell*, **33**, 299–311.
9. Foltz,D.R., Jansen,L.E., Bailey,A.O., Yates,J.R. 3rd, Bassett,E.A., Wood,S., Black,B.E. and Cleveland,D.W. (2009) Centromere-specific assembly of CENP-A nucleosomes is mediated by HJURP. *Cell*, **137**, 472–484.
10. Shuaib,M., Ouararhni,K., Dimitrov,S. and Hamiche,A. (2010) HJURP binds CENP-A via a highly conserved N-terminal domain and mediates its deposition at centromeres. *Proc. Natl. Acad. Sci. U.S.A.*, **107**, 1349–1354.
11. Chen,C.C., Dechassa,M.L., Bettini,E., Ledoux,M.B., Belisario,C., Huen,P., Luger,K. and Mellone,B.G. (2014) CAL1 is the Drosophila CENP-A assembly factor. *J. Cell Biol.*, **204**, 313–329.
12. Collins,K.A., Furuyama,S. and Biggins,S. (2004) Proteolysis contributes to the exclusive centromere localization of the yeast Cse4/CENP-A histone H3 variant. *Curr. Biol.*, **14**, 1968–1972.
13. Heun,P., Erhardt,S., Blower,M.D., Weiss,S., Skora,A.D. and Karpen,G.H. (2006) Mislocalization of the Drosophila centromere-specific histone CID promotes formation of functional ectopic kinetochores. *Dev. Cell*, **10**, 303–315.
14. Moreno-Moreno,O., Torras-Llort,M. and Azorin,F. (2006) Proteolysis restricts localization of CID, the centromere-specific histone H3 variant of Drosophila, to centromeres. *Nucleic Acids Res.*, **34**, 6247–6255.
15. Au,W.C., Crisp,M.J., DeLuca,S.Z., Rando,O.J. and Basrai,M.A. (2008) Altered dosage and mislocalization of histone H3 and Cse4p lead to chromosome loss in Saccharomyces cerevisiae. *Genetics*, **179**, 263–275.
16. Gonzalez,M., He,H., Dong,Q., Sun,S. and Li,F. (2014) Ectopic centromere nucleation by CENP-A in fission yeast. *Genetics*, **198**, 1433–1446.
17. Shrestha,R.L., Ahn,G.S., Staples,M.I., Sathyan,K.M., Karpova,T.S., Foltz,D.R. and Basrai,M.A. (2017) Mislocalization of centromeric histone H3 variant CENP-A contributes to chromosomal instability (CIN) in human cells. *Oncotarget*, **8**, 46781–46800.
18. Shrestha,R.L., Rossi,A., Wangsa,D., Hogan,A.K., Zaldana,K.S., Suva,E., Chung,Y.J., Sanders,C.L., Difilippantonio,S., Karpova,T.S., *et al.* (2021) CENP-A overexpression promotes aneuploidy with karyotypic heterogeneity. *J. Cell Biol.*, **220**, e202007195.
19. Shrestha,R.L., Balachandra,V., Kim,J.H., Rossi,A., Vadlamani,P., Sethi,S.C., Ozbun,L., Lin,S., Cheng,K.C., Chari,R., *et al.* (2023) The histone H3/H4 chaperone CHAF1B prevents the mislocalization of CENP-A for chromosomal stability. *J. Cell Sci.*, **136**, jcs260944.
20. Tomonaga,T., Matsushita,K., Yamaguchi,S., Oohashi,T., Shimada,H., Ochiai,T., Yoda,K. and Nomura,F. (2003) Overexpression and mistargeting of centromere protein-A in human primary colorectal cancer. *Cancer Res.*, **63**, 3511–3516.
21. Amato,A., Schillaci,T., Lentini,L. and Di Leonardo,A. (2009) CENPA overexpression promotes genome instability in pRb-depleted human cells. *Mol. Cancer*, **8**, 119.
22. Hu,Z., Huang,G., Sadanandam,A., Gu,S., Lenburg,M.E., Pai,M., Bayani,N., Blakely,E.A., Gray,J.W. and Mao,J.H. (2010) The expression level of HJURP has an independent prognostic impact and predicts the sensitivity to radiotherapy in breast cancer. *Breast Cancer Res.*, **12**, R18.
23. Li,Y., Zhu,Z., Zhang,S., Yu,D., Yu,H., Liu,L., Cao,X., Wang,L., Gao,H. and Zhu,M. (2011) ShRNA-targeted centromere protein A inhibits hepatocellular carcinoma growth. *PLoS One*, **6**, e17794.
24. Wu,Q., Qian,Y.M., Zhao,X.L., Wang,S.M., Feng,X.J., Chen,X.F. and Zhang,S.H. (2012) Expression and prognostic significance of centromere protein A in human lung adenocarcinoma. *Lung Cancer*, **77**, 407–414.
25. Lacoste,N., Woolfe,A., Tachiwana,H., Garea,A.V., Barth,T., Cantaloube,S., Kurumizaka,H., Imhof,A. and Almouzni,G. (2014) Mislocalization of the centromeric histone variant CenH3/CENP-A in human cells depends on the chaperone DAXX. *Mol. Cell*, **53**, 631–644.
26. Athwal,R.K., Walkiewicz,M.P., Baek,S., Fu,S., Bui,M., Camps,J., Ried,T., Sung,M.H. and Dalal,Y. (2015) CENP-A nucleosomes localize to transcription factor hotspots and subtelomeric sites in human cancer cells. *Epigenetics Chromatin*, **8**, 2.
27. Sun,X., Clermont,P.L., Jiao,W., Helgason,C.D., Gout,P.W., Wang,Y. and Qu,S. (2016) Elevated expression of the centromere protein-A(CENP-A)-encoding gene as a prognostic and predictive biomarker in human cancers. *Int. J. Cancer*, **139**, 899–907.
28. Hewawasam,G., Shivaraju,M., Mattingly,M., Venkatesh,S., Martin-Brown,S., Florens,L., Workman,J.L. and Gerton,J.L. (2010) Psh1 is an E3 ubiquitin ligase that targets the centromeric histone variant Cse4. *Mol. Cell*, **40**, 444–454.
29. Ranjitkar,P., Press,M.O., Yi,X., Baker,R., MacCoss,M.J. and Biggins,S. (2010) An E3 ubiquitin ligase prevents ectopic localization of the centromeric histone H3 variant via the centromere targeting domain. *Mol. Cell*, **40**, 455–464.
30. Ohkuni,K., Takahashi,Y., Fulp,A., Lawrimore,J., Au,W.C., Pasupala,N., Levy-Myers,R., Warren,J., Strunnikov,A., Baker,R.E., *et al.* (2016) SUMO-Targeted Ubiquitin Ligase (STUbL) Slx5 regulates proteolysis of centromeric histone H3 variant Cse4 and prevents its mislocalization to euchromatin. *Mol. Biol. Cell*, **27**, 1500–1510.
31. Cheng,H., Bao,X., Gan,X., Luo,S. and Rao,H. (2017) Multiple E3s promote the degradation of histone H3 variant Cse4. *Sci. Rep.*, **7**, 8565.
32. Ohkuni,K., Levy-Myers,R., Warren,J., Au,W.C., Takahashi,Y., Baker,R.E. and Basrai,M.A. (2018) N-terminal sumoylation of centromeric histone H3 variant Cse4 regulates its proteolysis to prevent mislocalization to non-centromeric chromatin. *G3*, **8**, 1215–1223.
33. Cheng,H., Bao,X. and Rao,H. (2016) The F-box protein Rcy1 is involved in the degradation of histone H3 variant Cse4 and genome maintenance. *J. Biol. Chem.*, **291**, 10372–10377.
34. Au,W.C., Zhang,T., Mishra,P.K., Eisenstatt,J.R., Walker,R.L., Ocampo,J., Dawson,A., Warren,J., Costanzo,M., Baryshnikova,A., *et al.* (2020) Skp, cullin, F-box (SCF)-Met30 and SCF-Cdc4-mediated proteolysis of CENP-A prevents mislocalization of CENP-A for chromosomal stability in budding yeast. *PLoS Genet.*, **16**, e1008597.
35. Ohkuni,K., Gliford,L., Au,W.C., Suva,E., Kaiser,P. and Basrai,M.A. (2022) Cdc48Ufd1/Npl4 segregase removes mislocalized centromeric histone H3 variant CENP-A from non-centromeric chromatin. *Nucleic Acids Res.*, **50**, 3276–3291.
36. Ohkuni,K., Abdulle,R. and Kitagawa,K. (2014) Degradation of centromeric histone H3 variant Cse4 requires the Fpr3 peptidyl-prolyl Cis-Trans isomerase. *Genetics*, **196**, 1041–1045.
37. Deyter,G.M. and Biggins,S. (2014) The FACT complex interacts with the E3 ubiquitin ligase Psh1 to prevent ectopic localization of CENP-A. *Genes Dev.*, **28**, 1815–1826.
38. Hewawasam,G.S., Mattingly,M., Venkatesh,S., Zhang,Y., Florens,L., Workman,J.L. and Gerton,J.L. (2014) Phosphorylation by casein kinase 2 facilitates Psh1 protein-assisted degradation of Cse4 protein. *J. Biol. Chem.*, **289**, 29297–29309.
39. Ciftci-Yilmaz,S., Au,W.C., Mishra,P.K., Eisenstatt,J.R., Chang,J., Dawson,A.R., Zhu,I., Rahman,M., Bilke,S., Costanzo,M., *et al.* (2018) A genome-wide screen reveals a role for the HIR histone

chaperone complex in preventing mislocalization of budding yeast CENP-A. *Genetics*, **210**, 203–218.
40. Eisenstatt,J.R., Boeckmann,L., Au,W.C., Garcia,V., Bursch,L., Ocampo,J., Costanzo,M., Weinreich,M., Sclafani,R.A., Baryshnikova,A., *et al.* (2020) Dbf4-dependent kinase (DDK)-mediated proteolysis of CENP-A prevents mislocalization of CENP-A in *Saccharomyces cerevisiae*. *G3*, **10**, 2057–2068.
41. Hewawasam,G.S., Dhatchinamoorthy,K., Mattingly,M., Seidel,C. and Gerton,J.L. (2018) Chromatin assembly factor-1 (CAF-1) chaperone regulates Cse4 deposition into chromatin in budding yeast. *Nucleic Acids Res.*, **46**, 4440–4455.
42. Ohkuni,K., Suva,E., Au,W.C., Walker,R.L., Levy-Myers,R., Meltzer,P.S., Baker,R.E. and Basrai,M.A. (2020) Deposition of centromeric histone H3 variant CENP-A/Cse4 into chromatin is facilitated by its C-terminal sumoylation. *Genetics*, **214**, 839–854.
43. Eisenstatt,J.R., Ohkuni,K., Au,W.C., Preston,O., Gliford,L., Suva,E., Costanzo,M., Boone,C. and Basrai,M.A. (2021) Reduced gene dosage of histone H4 prevents CENP-A mislocalization and chromosomal instability in *Saccharomyces cerevisiae*. *Genetics*, **218**, iyab033.
44. Malik,N., Dantu,S.C., Shukla,S., Kombrabail,M., Ghosh,S.K., Krishnamoorthy,G. and Kumar,A. (2018) Conformational flexibility of histone variant CENP-A(Cse4) is regulated by histone H4: a mechanism to stabilize soluble Cse4. *J. Biol. Chem.*, **293**, 20273–20284.
45. Zhou,Z., Feng,H., Zhuou,B.-R., Ghirlando,R., Hu,K., Zwolak,A., Miller Jenkins,L.M., Xiao,H., Tjandra,N., Wu,C., *et al.* (2011) Structural basis for recognition of centromere histone variant CenH3 by the chaperone Scm3. *Nature*, **472**, 234–237.
46. Ohkuni,K., Takahashi,Y. and Basrai,M.A. (2015) Protein purification technique that allows detection of sumoylation and ubiquitination of budding yeast kinetochore proteins Ndc10 and Ndc80. *J. Vis. Exp.*, **99**, e52482.
47. Hildebrand,E.M. and Biggins,S. (2016) Regulation of budding yeast CENP-A levels prevents misincorporation at promoter nucleosomes and transcriptional defects. *PLoS Genet.*, **12**, e1005930.
48. Glowczewski,L., Yang,P., Kalashnikova,T., Santisteban,M.S. and Smith,M.M. (2000) Histone-histone interactions and centromere function. *Mol. Cell. Biol.*, **20**, 5700–5711.
49. Deyter,G.M., Hildebrand,E.M., Barber,A.D. and Biggins,S. (2017) Histone H4 facilitates the proteolysis of the budding yeast CENP-ACse4 centromeric histone variant. *Genetics*, **205**, 113–124.

Received: August 23, 2023. **Revised:** October 27, 2023. **Editorial Decision:** November 1, 2023. **Accepted:** November 9, 2023
Published by Oxford University Press on behalf of Nucleic Acids Research 2023.
This work is written by (a) US Government employee(s) and is in the public domain in the US.